

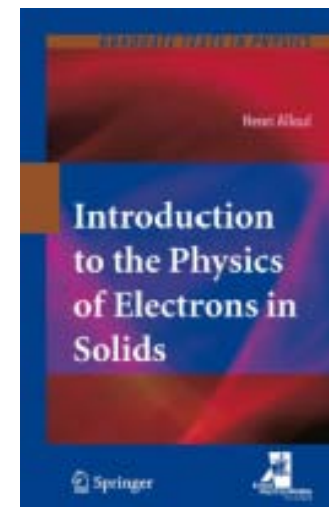


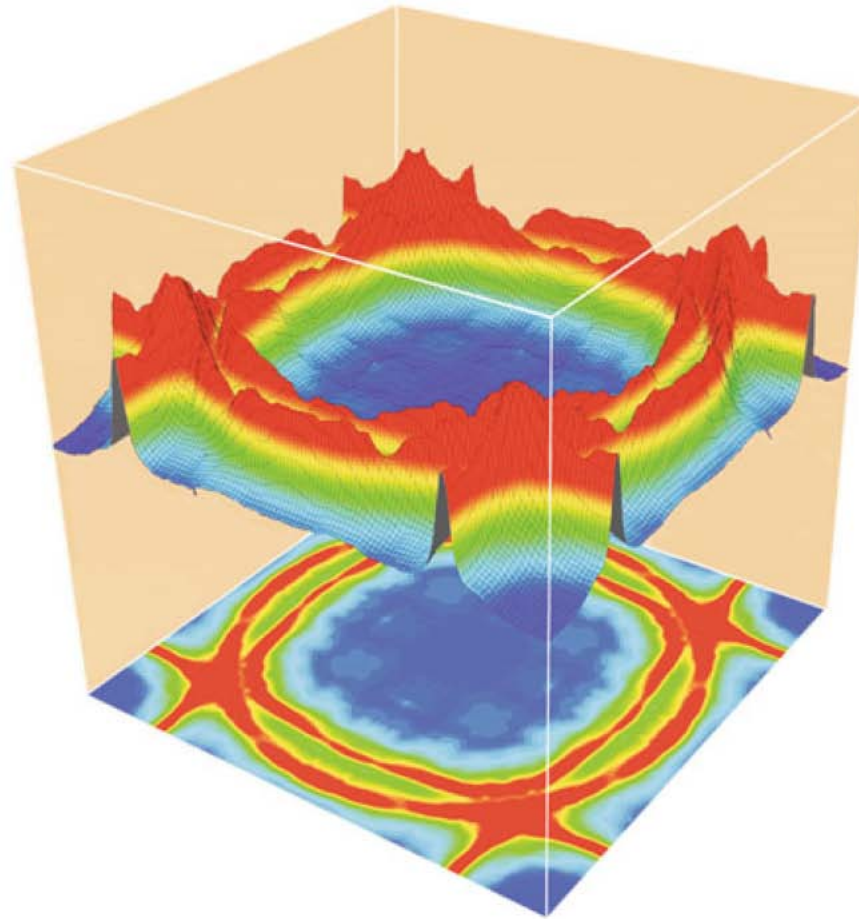
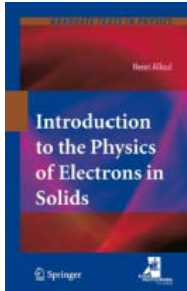
Advanced solid state physics

Alloul, Introduction to the Physics of Electrons in Solids, Springer-Verlag Berlin Heidelberg 2011

the Fermi surface of a metallic material can be represented in reciprocal space using angle-resolved photoemission experiments. In this image, the Fermi surface of the CuO_2 plane of the cuprate superconductor $\text{BiSr}_2\text{CaCu}_2\text{O}_8$ is reconstructed experimentally in the reciprocal space plane k_x, k_y

from





Experimental observation of the electronic states of Sr_2RuO_4 obtained by Angular Resolved Photoemission Spectroscopy (ARPES), a technique that takes benefit from the intense monochromatic light beams produced by synchrotrons. This technique has been intensively developed since the 1990s in particular for the study of high temperature superconductors.

Energy Bands in Solids-what are they good for?

1. Is the material a metal, a semiconductor (direct or indirect gap), semimetal or insulator?
2. To which atomic (molecular) levels do the bands on the band diagram correspond? Which bands are important in determining the electronic structure? What are the bandwidths, bandgaps?

What information does $E(\vec{k})$ diagram provide concerning the following questions:

- (a) Where are the carriers in the Brillouin zone?
- (b) Are the carriers electrons or holes?
- (c) Are there many or few carriers?
- (d) How many carrier pockets of each type are there in the Brillouin zone?
- (e) What is the shape of the Fermi surface?
- (f) Are the carrier velocities high or low?
- (g) Are the carrier mobilities for each carrier pocket high or low?

Goal: Calculate electrical properties (eg. resistance) for solids

Approach:

• Macroscopic theory: V, I, R

$$V = IR$$

• Microscopic theory: J, E, σ

$$\mathbf{J} = \sigma \mathbf{E}$$

$$\frac{l}{\sigma A} = R$$

• Phenomenological model of transport: n, τ, m

$$\sigma = \frac{ne^2\tau}{m}$$

• Relate parameters in phenomenological theory to electronic energy levels and wavefunction

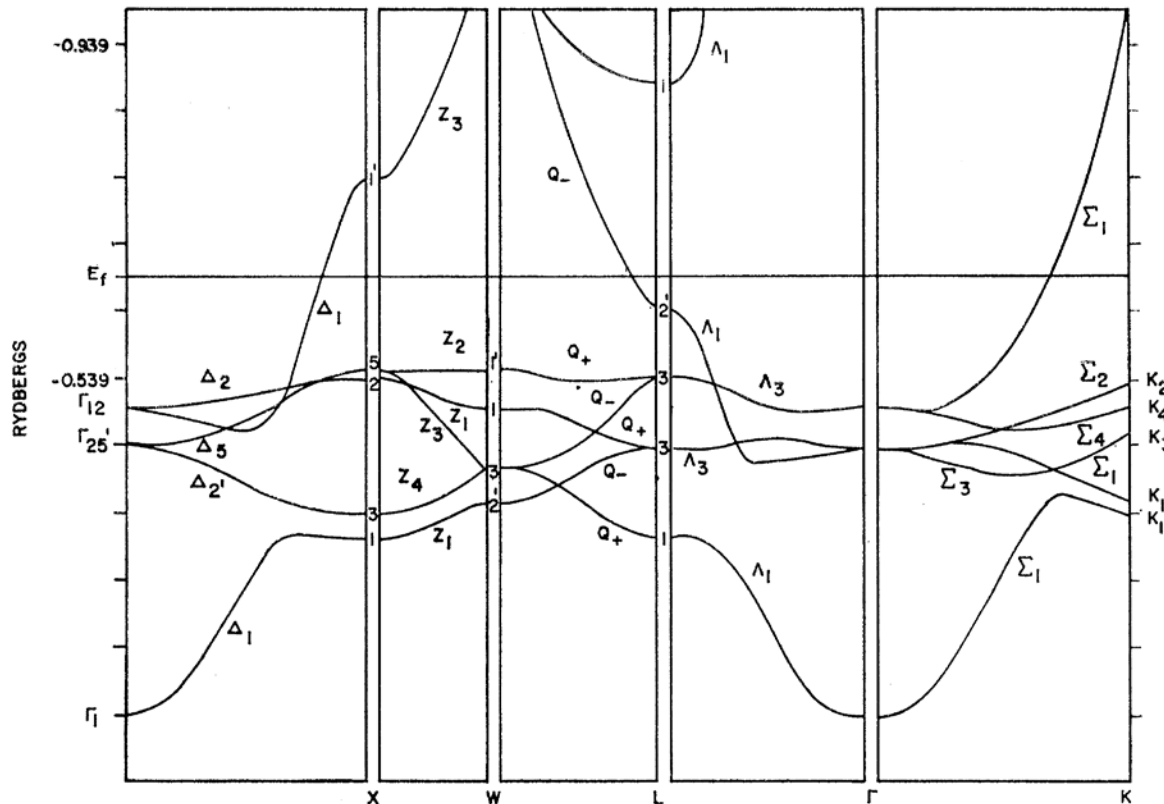
You will be able to relate a bandstructure to macroscopic parameters for the solid

$$\sigma = e^2 v_F^2 \tau g(E_F)$$

$$C_V = \left. \frac{\partial ((E/V))}{\partial T} \right|_{V,N} = \frac{\pi^2}{3} k_B^2 T g(E_{F0}) = \gamma T$$

Density of States is the Central Character in this Story

In the case of copper, the bands near the Fermi level are derived from the 4s and 3d atomic levels. The so-called 4s and 3d bands accommodate a total of 12 electrons, while the number of available electrons is 11. Therefore the Fermi level must cross these bands. Consequently copper is metallic.



Some pictures are taken from Ashcroft and Mermin from Kittel from Mizutani and from several sources on the web.

Experimental techniques and principles of electronic structure-related phenomena

de Haas–van Alphen effect

Positron annihilation

Compton scattering effect

Photoemission spectroscopy

Inverse photoemission spectroscopy

Angular-resolved photoemission spectroscopy (ARPES)

Soft x-ray spectroscopy

Electron-energy-loss spectroscopy (EELS)

Optical reflection and absorption spectra

INTRODUCTION TO THE ELECTRON
THEORY OF METALS

UICHIRO MIZUTANI

This edition © Cambridge University Press (Virtual Publishing) 2003

the determination of the Fermi surface topology.

recognized as one of the most powerful and accurate methods

de Haas–van Alphen effect

Quantum oscillations and the topology of Fermi surfaces

The conduction electron moving with the velocity \mathbf{v} in the presence of electrical and magnetic fields experiences the **Lorentz force** given by

$$\mathbf{F} = (-e)(\mathbf{E} + \mathbf{v} \times \mathbf{B})$$

$$\mathbf{F} = (-e)(\mathbf{E} + \mathbf{v} \times \mathbf{B})$$

In this section, we ignore the first term and consider only the effect of the magnetic field on the motion of the conduction electron.

the electron rotates in a closed orbit, if the velocity \mathbf{v} has no component along the magnetic field \mathbf{B} . If there is a non-zero component of the velocity in the direction of \mathbf{B} , the electron will be subjected to a helical motion.

- In any event, the magnetic field alters the direction of \mathbf{v} but not its magnitude.
- Thus, the energy of the electron is kept unchanged.

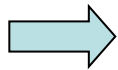
the force \mathbf{F} exerted on the Bloch electron of wave vector \mathbf{k}

$$\frac{\hbar d\mathbf{k}}{dt} = (-e)(\mathbf{v} \times \mathbf{B})$$

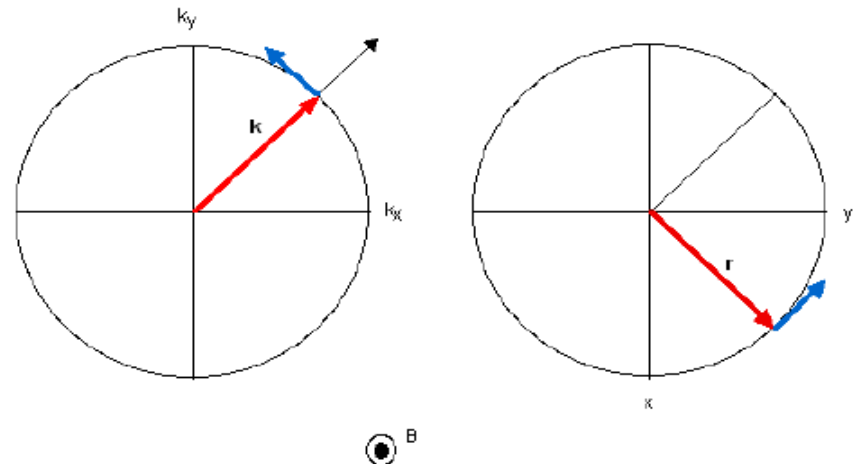
$$\frac{\hbar d\mathbf{k}}{dt} = (-e)(\mathbf{v} \times \mathbf{B})$$

the motion of an electron of wave vector \mathbf{k} can be described in reciprocal space as rotating in a closed orbit on a constant energy surface normal to the magnetic field \mathbf{B} .

integrating



$$\mathbf{k} - \mathbf{k}_0 = \left(\frac{(-e)}{\hbar} \right) (\mathbf{r} \times \mathbf{B})$$



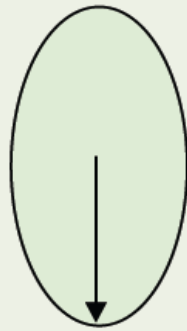
means that the trajectory of the electron in reciprocal space has the same shape as that in real space but is rotated by 90° and scaled by the factor $(-e)B/\hbar$.

(S.I.)

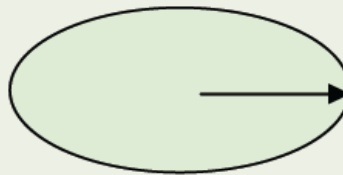
$$\hbar \dot{\vec{k}} = -\frac{e}{c} \dot{\vec{r}} \times \vec{B} \quad \rightarrow \quad \dot{\vec{r}} = -\frac{\hbar c}{eB^2} \vec{B} \times \dot{\vec{k}}$$

$$\rightarrow \quad \vec{r}(t) - \vec{r}(0) = -\frac{\hbar c}{eB} \hat{B} \times [\vec{k}(t) - \vec{k}(0)] \quad (\text{CGS})$$

r-orbit



k-orbit



r-orbit is rotated by 90 degrees from the k-orbit and scaled by $\hbar c/eB \equiv \lambda_B^2$

magnetic length $\lambda_B = 256 \text{ \AA}$ at $B = 1 \text{ Tesla}$

The closed orbit of the Bloch electron in the magnetic field is quantized in the same manner as the electron orbit of a free atom. The Bohr–Sommerfeld quantization rule for the motion of the Bloch electron in the magnetic field is explicitly written as

$$\oint (\hbar \mathbf{k} + (-e)\mathbf{A}) d\mathbf{s} = \left(n + \frac{1}{2} \right) h$$

Using the Gauss theorem

$$(-e) \oint \mathbf{A} d\mathbf{s} = (-e) \iint \text{rot} \mathbf{A} d\mathbf{S} = (-e) \iint \mathbf{B} d\mathbf{S} = (-e) B S.$$

with

$$\mathbf{k} - \mathbf{k}_0 = \left(\frac{(-e)}{\hbar} \right) (\mathbf{r} \times \mathbf{B}), \quad \mathbf{k}_0 = 0$$

$$\oint \hbar \mathbf{k} d\mathbf{s} = -(-e) \mathbf{B} \cdot \oint \mathbf{r} \times d\mathbf{s} = -2(-e) B S.$$

in

$$\oint (\hbar \mathbf{k} + (-e) \mathbf{A}) d\mathbf{s} = \left(n + \frac{1}{2} \right) h$$

$$e B S = \left(n + \frac{1}{2} \right) h$$

Let us denote the area of the closed orbit in reciprocal space as $A(\varepsilon)$

We get

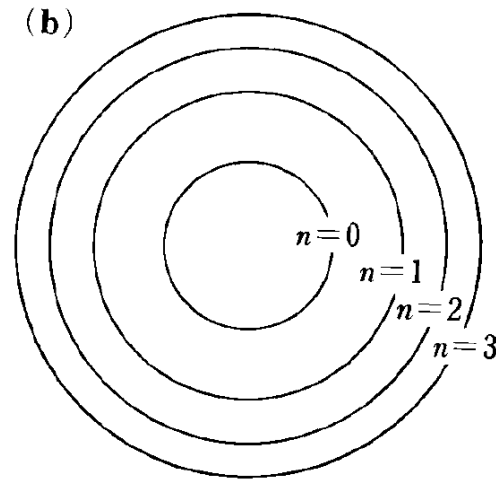
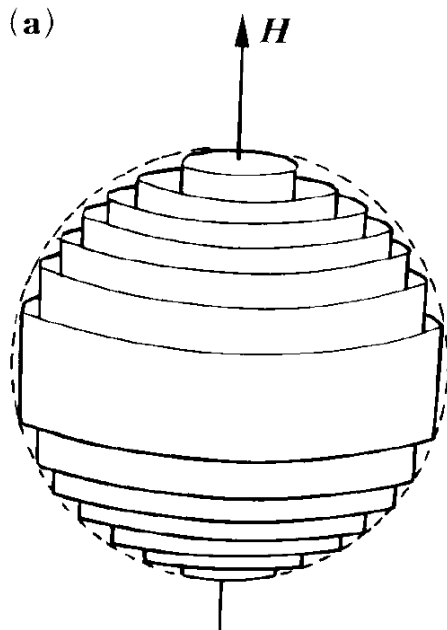
$$A(\varepsilon) = \left(\frac{eB}{\hbar} \right)^2 S.$$

$$\mathbf{k} - \mathbf{k}_0 = \left(\frac{(-e)}{\hbar} \right) (\mathbf{r} \times \mathbf{B})$$

$$A_n(\varepsilon) = \left(\frac{2\pi e B}{\hbar} \right) \left(n + \frac{1}{2} \right)$$

$$A_n(\epsilon) = \left(\frac{2\pi e B}{\hbar} \right) \left(n + \frac{1}{2} \right)$$

three independent quantum numbers k_x , k_y and k_z of the wave vector \mathbf{k} are reduced to two quantum numbers n and k_z in the presence of a magnetic field along the z -axis.

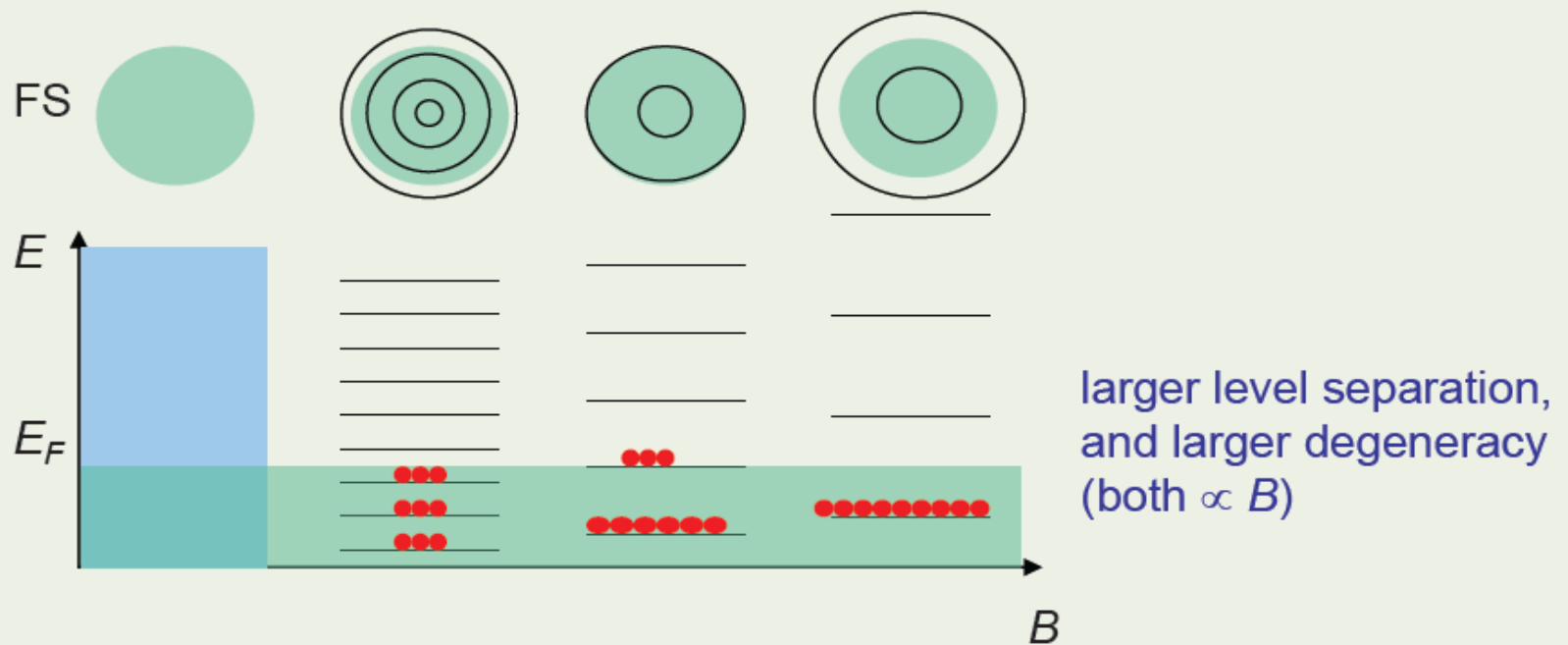


from
Mizutani

(a) The free-electron Fermi surface in the presence of a magnetic field along the z -axis. (b) Its projection onto the $k_x k_y$ -plane.

Note:

1. In the presence of B , the Fermi sphere becomes a stack of cylinders.
2. Fermi energy ≈ 1 eV, cyclotron energy ≈ 0.1 meV (for $B = 1$ T)
 \therefore the number of cylinders usually ≈ 10000 !
 need low T and high B to observe the fine structure
3. Radius of cylinders $\propto \sqrt{B}$, so they expand as we increase B .
 The orbits are pushed out of the FS one by one.



- Successive B 's that produce orbits with the same area: (CGS)

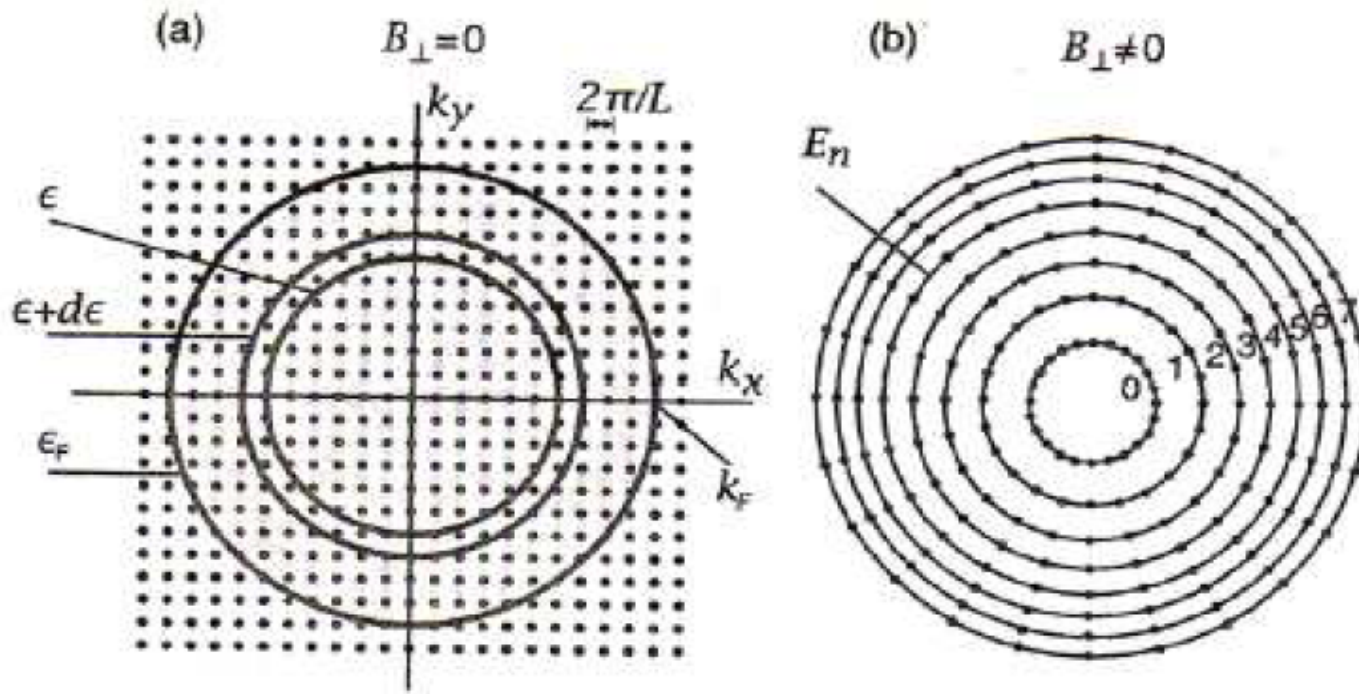
$$S_n = (n+1/2) 2\pi e/\hbar c B$$

$$S_{n'} = (n-1/2) 2\pi e/\hbar c B' \quad (B' > B)$$

$$S\left(\frac{1}{B} - \frac{1}{B'}\right) = \frac{2\pi e}{\hbar c}$$

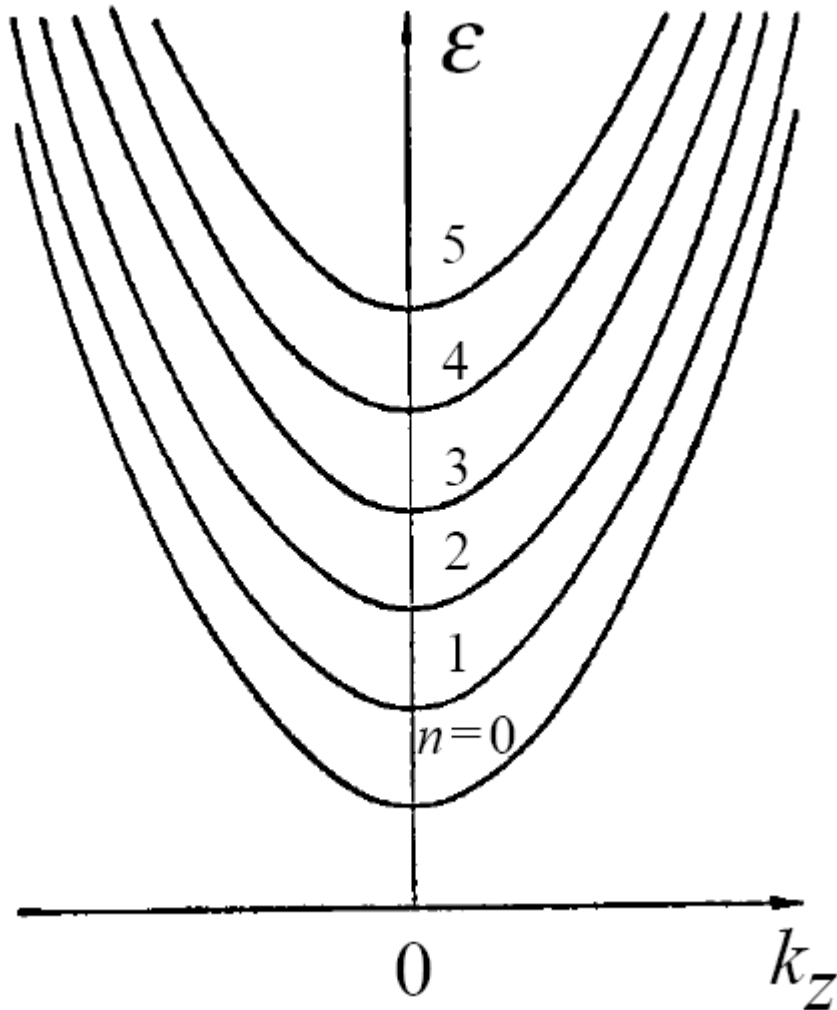
equal increment of $1/B$ reproduces similar orbits

reciprocal space



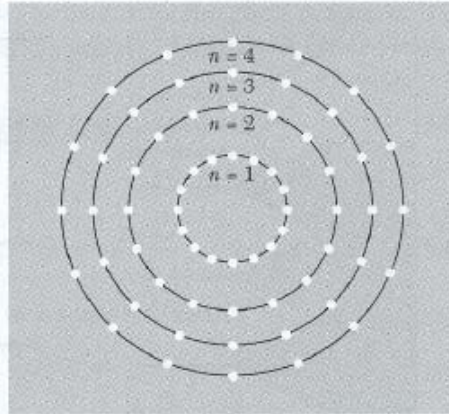
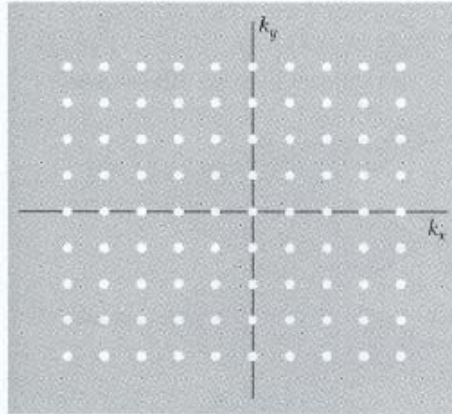
Quantization scheme for free electrons. Electron states are denoted by points in the \mathbf{k} space in the absence and presence of external magnetic field \mathbf{B} . The states on each circle are degenerate. (a) When $\mathbf{B} = 0$, there is one state per area $(2\pi/L)^2$. (b) When $\mathbf{B} \neq 0$, the electron energy is quantized into Landau levels. Each circle represents a Landau level with energy $E_n = \hbar\omega_c(n + 1/2)$.

$$\varepsilon = \left(n + \frac{1}{2}\right) \hbar \omega_c + \frac{\hbar^2 k_z^2}{2m} \quad (n=0, 1, 2, \dots) \quad \omega_c = eB/m$$



Landau levels

Condensation of States

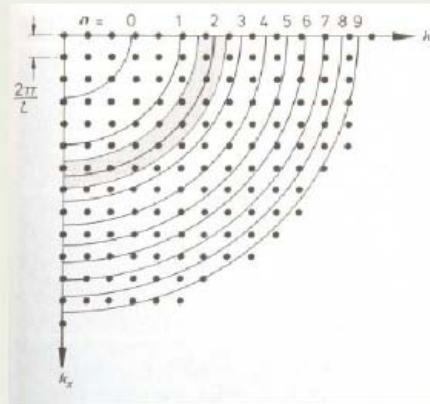


$$\Delta S = S_n - S_{n-1} = \frac{2\pi eB}{\hbar c} \quad (\text{CGS})$$

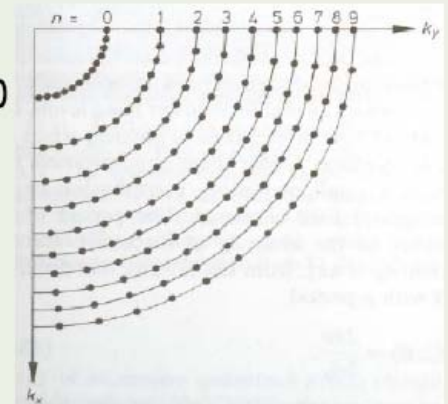
$$D = \frac{2\pi eB}{\hbar c} \left(\frac{L}{2\pi} \right)^2$$

The number of free electron orbital that coalesce in a single magnetic level

$B=0$

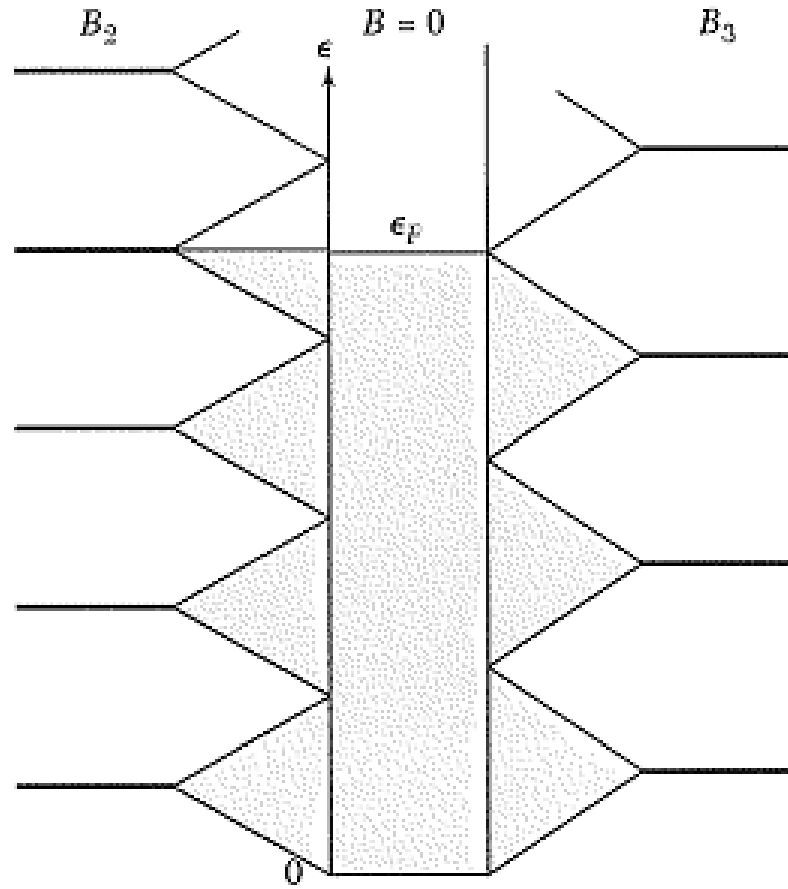
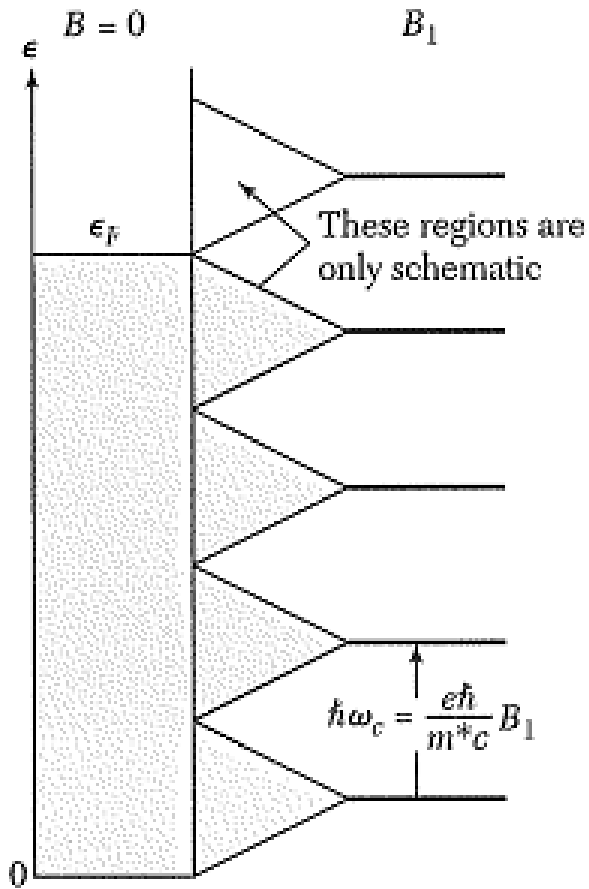


$B \neq 0$



De Haas-van Alphen Effect

dHvA effect: \mathbf{M} of a pure metal at low T in strong \mathbf{B} is a periodic function of $1/B$.



2-D e -gas

$$\Delta S = S_n - S_{n-1} = \frac{2\pi eB}{\hbar c}$$

(CGS)

$$\# \text{ of states in each Landau level} = D = \frac{2\pi eB}{\hbar c} \left(\frac{L}{2\pi} \right)^2 = \rho B$$

$$\rho = \frac{eL^2}{2\pi\hbar c}$$

Change in energy
distribution of conduction
electrons

The internal energy U of the
conduction electrons
depends critically on the
closeness of the highest
occupied Landau level to
the Fermi level E

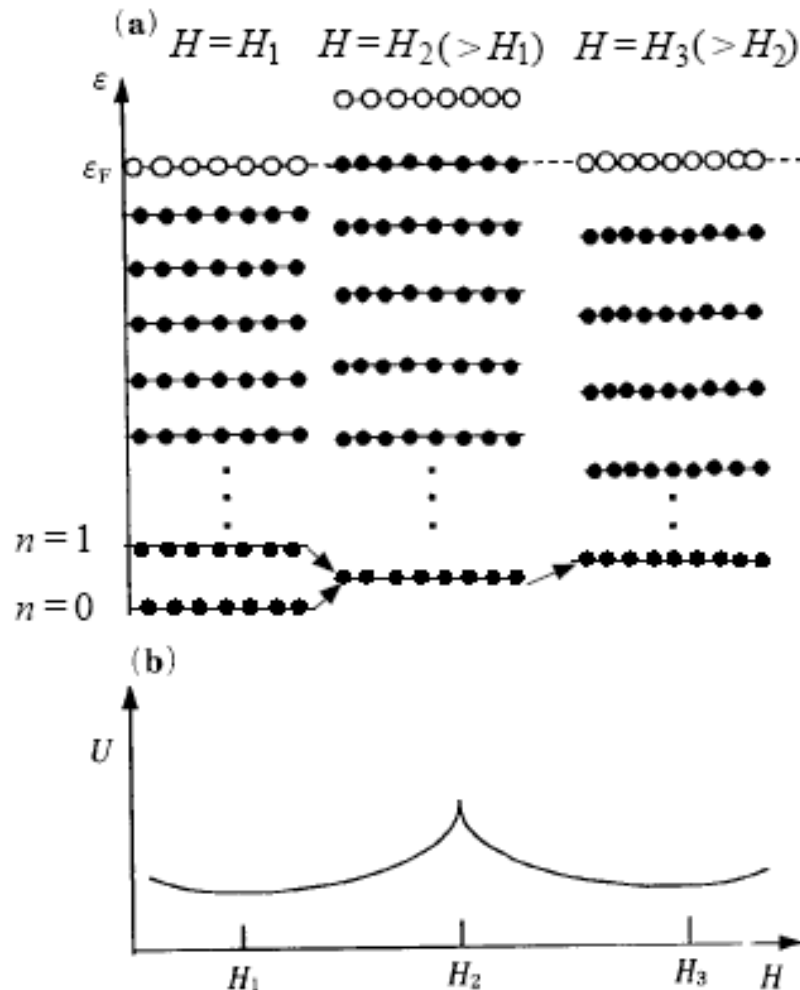


Figure 7.3. (a) Magnetic field dependence of the Landau level at absolute zero. With increasing magnetic field, the separation between the adjacent levels is widened and the population of electrons marked by solid circles in each level increases. The Landau level with $n=0$ is shown to be raised with increasing magnetic field. (b) Corresponding change in the internal energy.

Let us denote magnetic fields as $B_1 (= \mu_0 H_1)$ and $B_2 (= \mu_0 H_2)$, when the two successive Landau levels n and $n-1$ pass the Fermi level.

In Fermi surface experiments we may be interested in the increment ΔB for which two successive orbits, n and $n + 1$, have the same area in \mathbf{k} space on the Fermi surface. The areas are equal when

$$A(\varepsilon) \left(\frac{1}{B_1} - \frac{1}{B_2} \right) = \frac{2\pi e}{\hbar}$$

$$\Delta \left(\frac{1}{B} \right) = \frac{1}{B_1} - \frac{1}{B_2} = \frac{2\pi e}{\hbar A(\varepsilon)}.$$

Magnetic moment:

$$\mu = - \frac{\partial U}{\partial B}$$

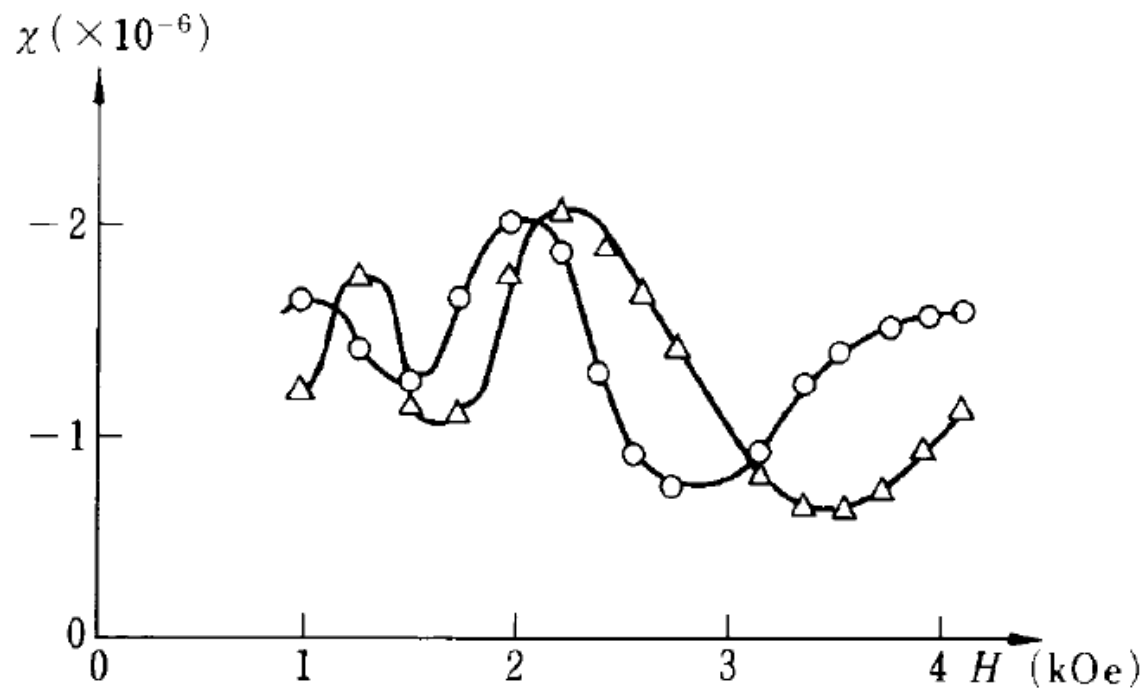


Figure 7.4. Oscillatory behavior of the magnetic susceptibility of a Bi single crystal measured by de Haas and van Alphen in 1930. Open circle and triangle refer to the data when the magnetic field is applied parallel to and perpendicular to the two-fold axis of the sample, respectively. The measuring temperature was 14.2 K. [W. J. de Haas and P. M. van Alphen, *Communications from the Physical Laboratory at the University of Leiden* **212a** (1930) 3]

De Haas – van Alphen Oscillations

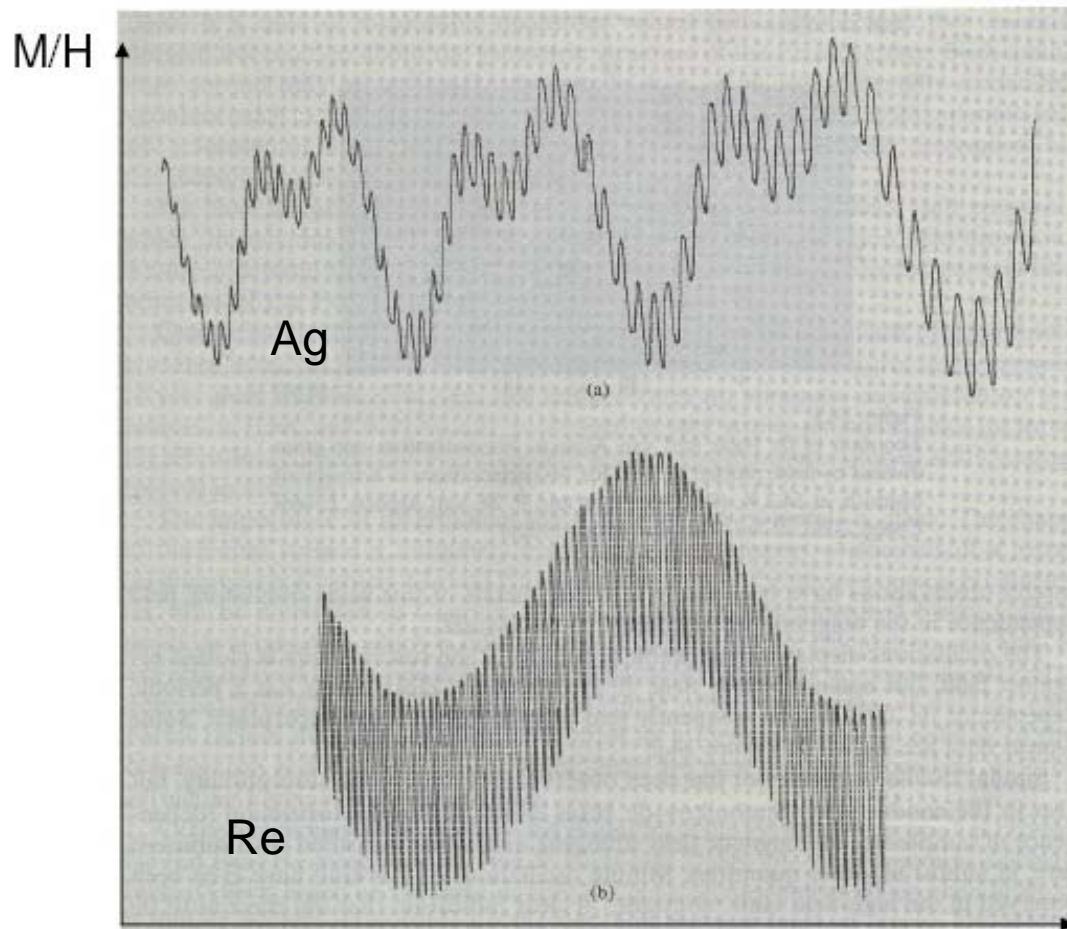
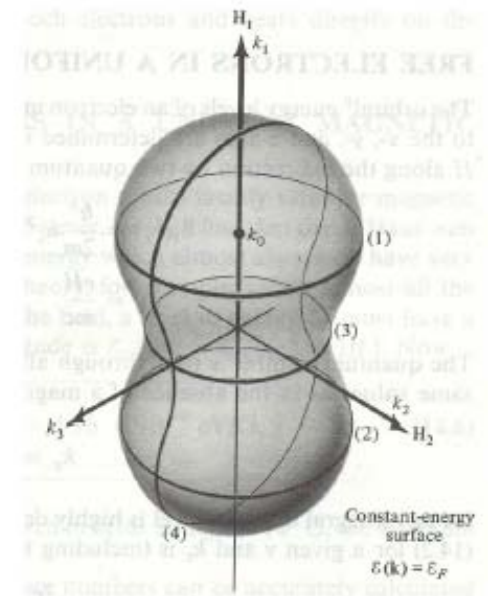


Figure 14.2
De Haas–van Alphen oscillations in (a) rhenium and (b) silver. (Courtesy of A. S. Joseph.)



$$\Delta\left(\frac{1}{H}\right) = \frac{2\pi e}{hc} \frac{1}{S_e}$$

Extremal Orbits. One point in the interpretation of the dHvA effect is subtle. For a Fermi surface of general shape the sections at different values of k_B will have different periods. The response will be the sum of contributions from all sections or all orbits. *But the dominant response of the system comes from orbits whose periods are stationary with respect to small changes in k_B .*

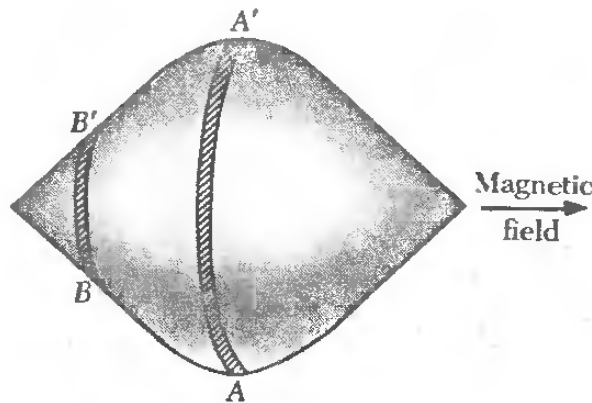
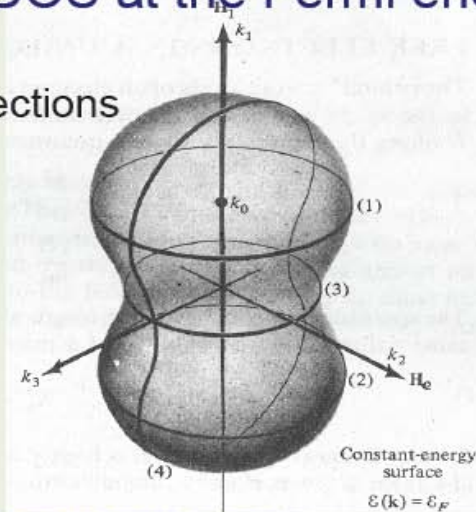


Figure 28 The orbits in the section AA' are extremal orbits: the cyclotron period is roughly constant over a reasonable section of the Fermi surface. Other sections such as BB' have orbits that vary in period along the section.

Oscillation of the DOS at the Fermi energy

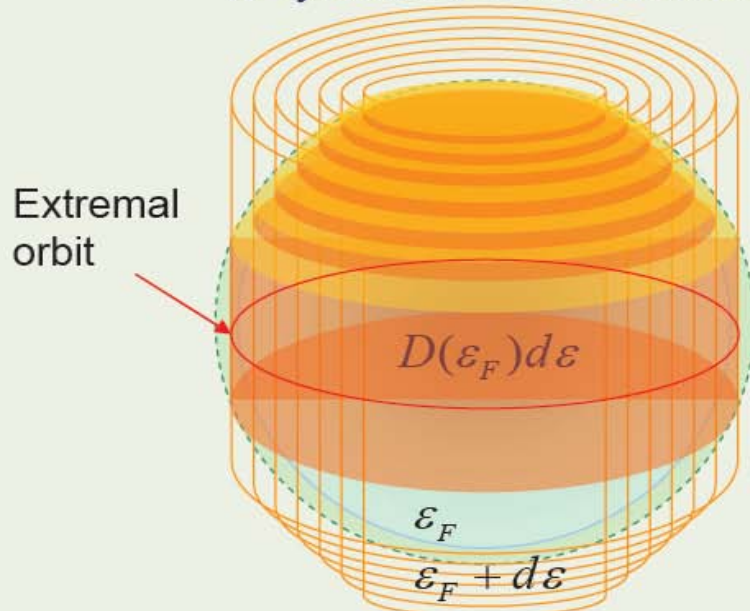
Max and min cross sections
(Extremal orbits)

Two extremal orbits

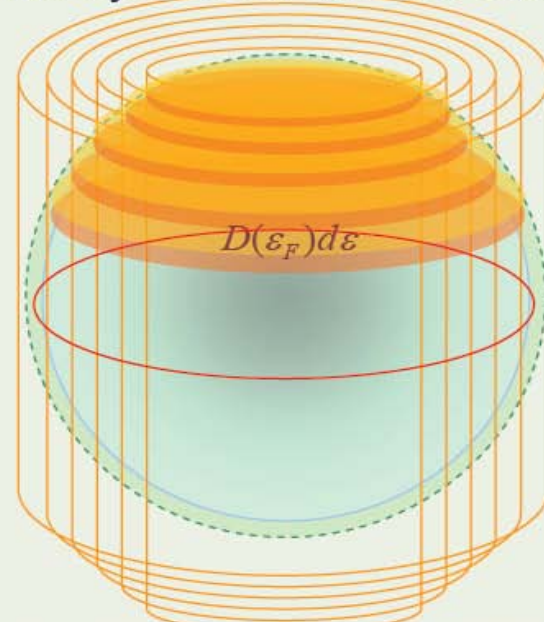


- The number of states at E_F are highly enhanced when there are extremal orbits on the FS
- There are extremal orbits at regular interval of $1/B$
- This oscillation in $1/B$ can be detected in any physical quantity that depends on the DOS

A cylinder on extremal orbit



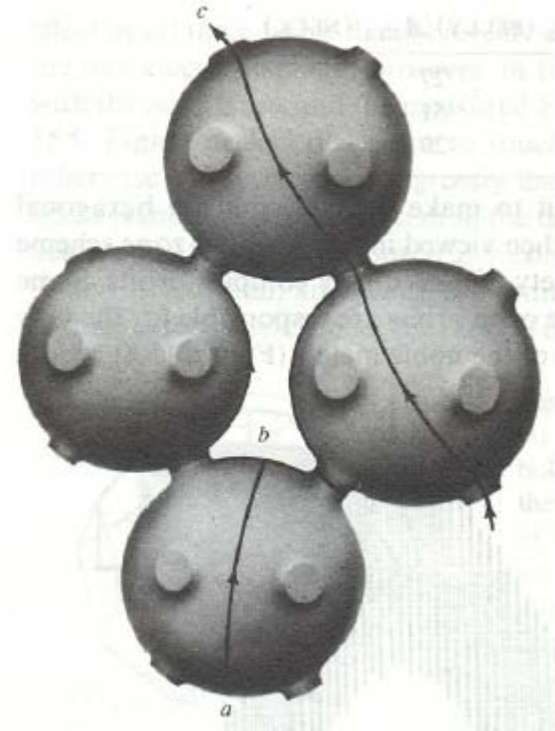
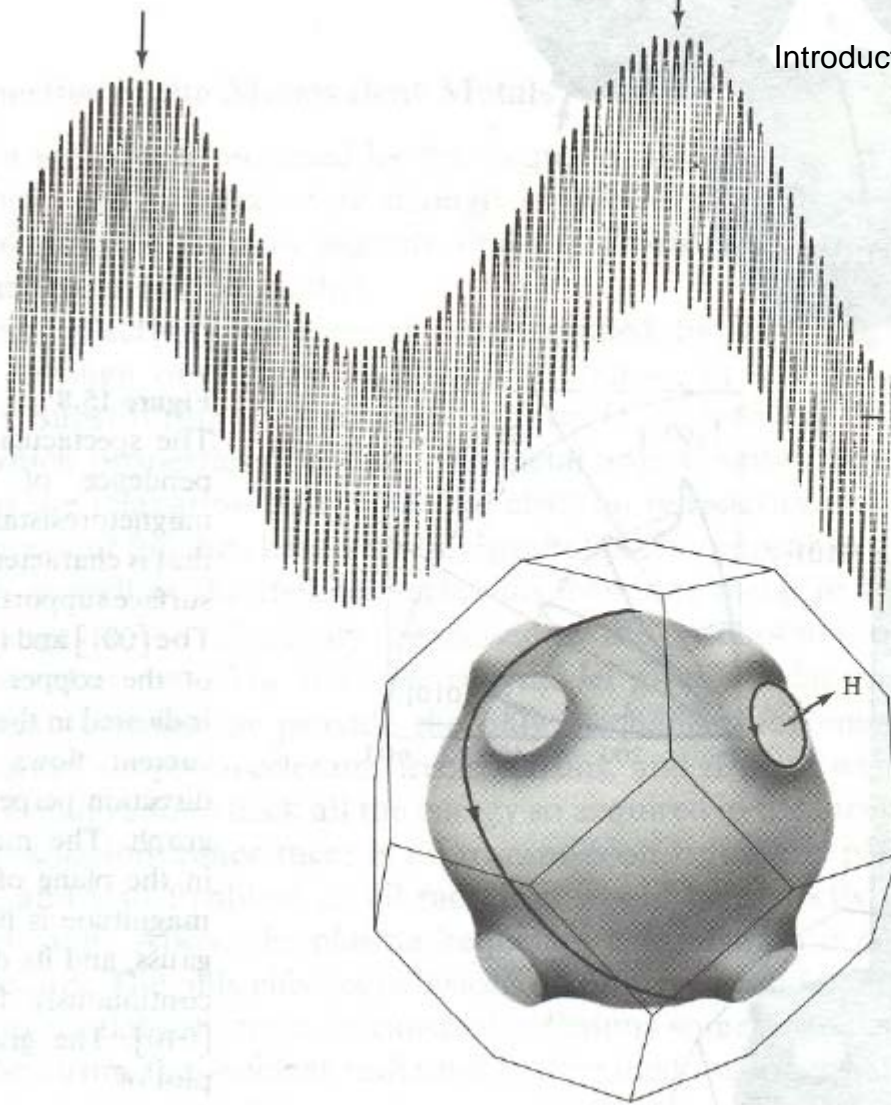
No cylinder on extremal orbit



Number of states is proportional to area of cylinders in spherical shell

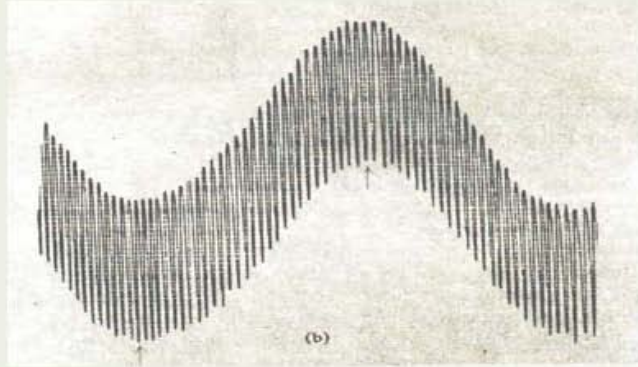
De Haas- van Alphen oscillation - Copper

Introduction to solid state physics WS 2005/06 M. Wolf



the detailed structure of the Fermi surface of Cu, Ag and Au has been accurately determined from the measurement of the de Haas-van Alphen effect

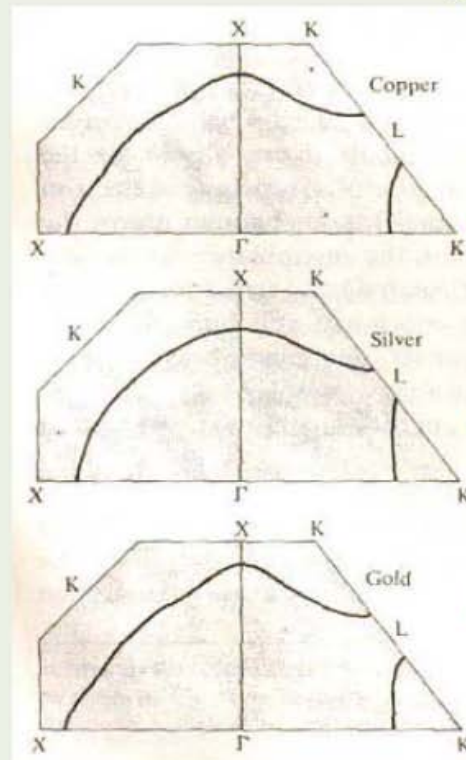
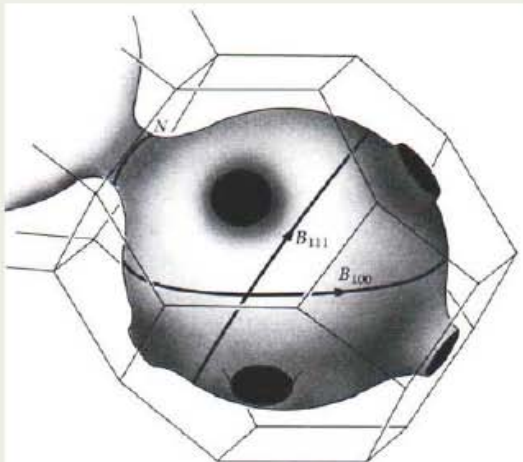
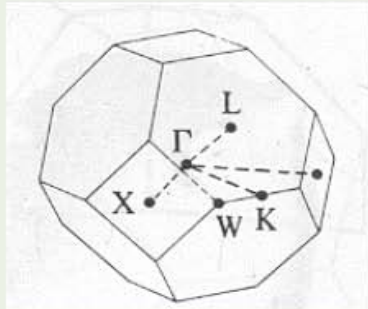
Determination of FS



In the dHvA experiment of silver, the two different periods of oscillation are due to two different extremal orbits

$$\text{Recall that } S_e \left(\frac{1}{B} - \frac{1}{B'} \right) = \frac{2\pi e}{\hbar c}$$

Therefore, from the two periods we can determine the ratio between the sizes of the "neck" and the "belly"



$$A_{111}(\text{belly})/A_{111}(\text{neck})=27$$

$$A_{111}(\text{belly})/A_{111}(\text{neck})=51$$

$$A_{111}(\text{belly})/A_{111}(\text{neck})=29$$

The de Haas-van Alphen effect is the oscillation of the magnetic moment of a metal as a function of the static magnetic field intensity. The effect can be observed in pure specimens at low temperatures in strong magnetic fields; we do not want the quantization of the electron orbits to be blurred by collisions, and we do not want the population oscillations to be averaged out by thermal population of adjacent orbits.

very pure samples at low temperatures

(C. Kittel)

Experimental

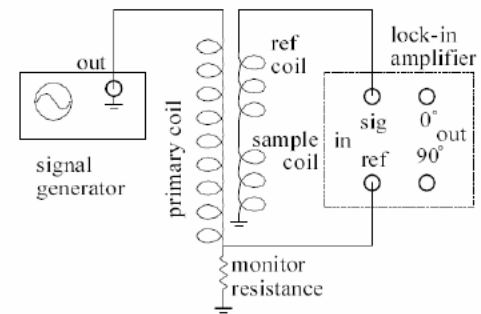
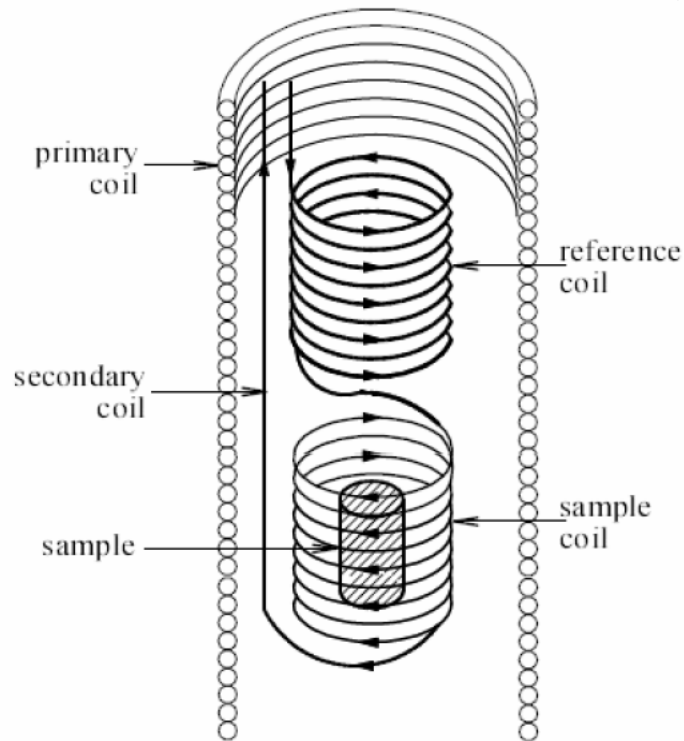
Field-modulation method

The system consists of a detecting coil, a compensation coil, and a field modulation coil. The static magnetic field B (superconducting magnet or ion core magnet) is modulated by a small AC field $h_0 \cos \omega t$ (ω is a angular frequency) generated by the field modulation coil. The direction of the AC field is parallel to that of a static magnetic field B . The voltage induced in the pick-up coil is given by

$$v \propto \omega \left\{ h \frac{\partial M}{\partial h} \sin(\omega t) + \frac{1}{2} h^2 \sin(2\omega t) \frac{\partial^2 M}{\partial h^2} + \dots \right\}, \quad (10)$$

where $h \ll B$. The signal obtained from the pick-up coil is phase sensitively detected at the first harmonic or second harmonic modes with a lock-in amplifier. The DC signal is proportional to $\omega h \frac{\partial M}{\partial h}$ for the first-harmonic mode and $\omega h^2 \frac{\partial^2 M}{\partial h^2}$ for the second-harmonic mode. These signals are periodic in $1/B$. The Fourier analysis leads to the dHvA frequency F (or the dHvA period $P = 1/F$).

<http://www.binghamton.edu/physics/docs/note-dhva.pdf>



$$H = H_{dc} + H_{ac} \cos(\omega t)$$

Owing to the possession of small Fermi surfaces, de Haas and van Alphen were able to measure in 1930, for the first time, the oscillatory magnetic susceptibility with increasing applied magnetic field for a Bi single crystal

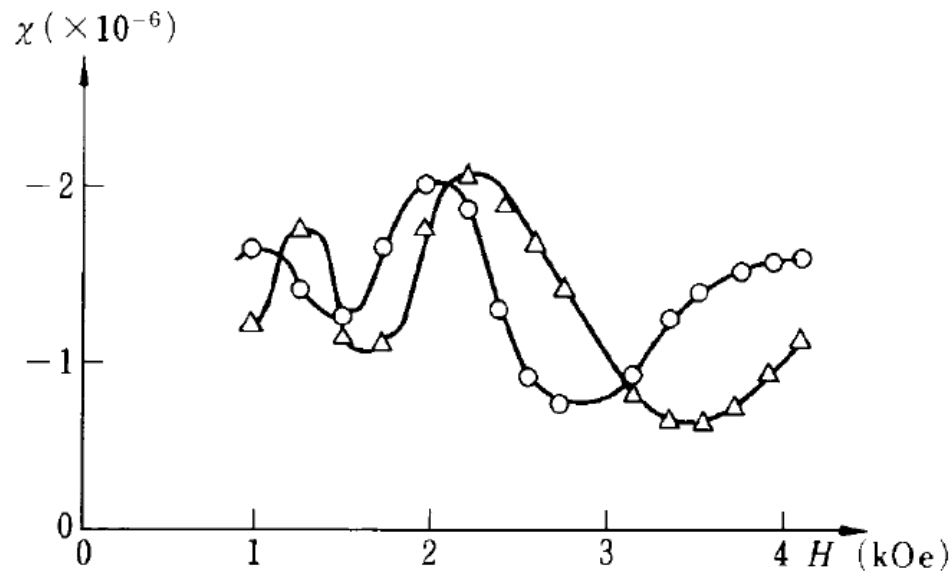


Figure 7.4. Oscillatory behavior of the magnetic susceptibility of a Bi single crystal measured by de Haas and van Alphen in 1930. Open circle and triangle refer to the data when the magnetic field is applied parallel to and perpendicular to the two-fold axis of the sample, respectively. The measuring temperature was 14.2 K. [W. J. de Haas and P. M. van Alphen, *Communications from the Physical Laboratory at the University of Leiden* **212a** (1930) 3]

from Mizutani

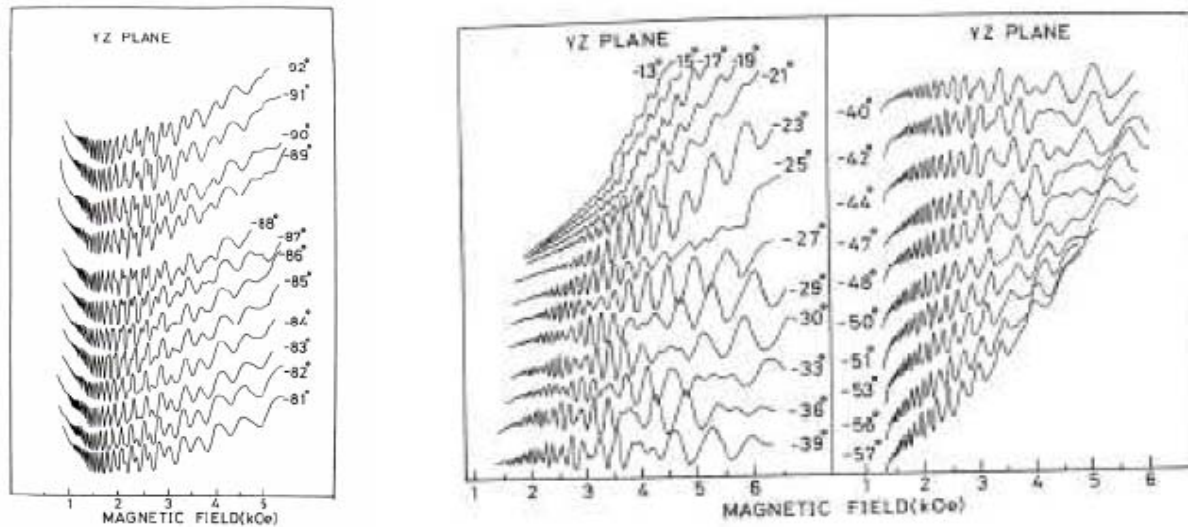
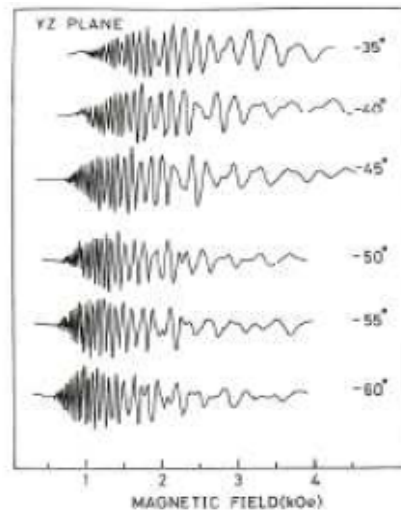


Fig.7 The dHvA effect of Bi in the YZ plane. $T = 1.5$ K. This signal corresponds to the first harmonics ($\partial M / \partial h$).

<http://www.binghamton.edu/physics/docs/note-dhva.pdf>



The dHvA effect of Bi in the YZ plane. $T = 1.5$ K. The signal corresponds to the second harmonics ($\partial^2 M / \partial h^2$).

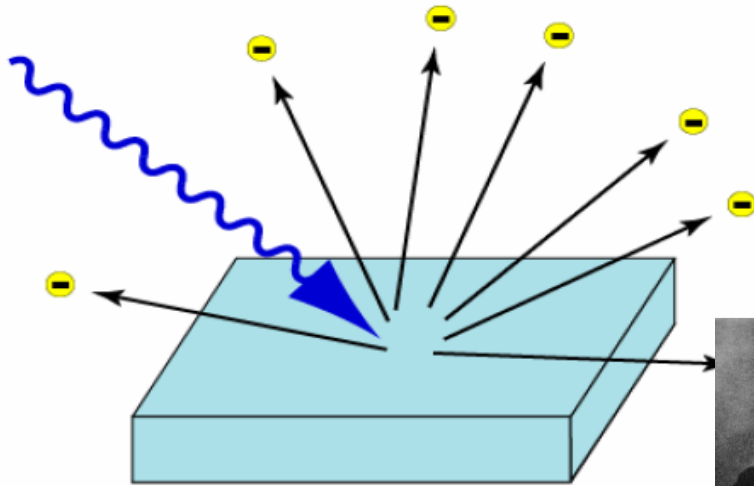
The oscillating internal energy of the conduction electron system is reflected in various electronic properties. The magnetic susceptibility is given by the differentiation of the internal energy with respect to the magnetic field. Hence, the magnetic susceptibility oscillates as a function of the magnetic field. This is the dHvA effect. The specific heat is derived from the differentiation of the internal energy with respect to temperature. Hence, the specific heat also oscillates with increasing magnetic field. This is known as magneto-thermal oscillation. The de Haas–Shubnikov effect refers to the oscillations of the electrical resistivity as a function of a magnetic field. Similarly, an oscillatory behavior is observed in the Hall coefficient and the thermoelectric power. The present discussion of the dHvA effect is rather qualitative.

from Mizutani

Photoemission spectroscopy

The Photoelectric Effect

see "Introduction to Photoemission Spectroscopy" Michael Sing
<http://www.cond-mat.de/events/correl14/talks/sing.pdf>



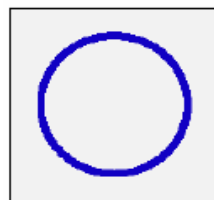
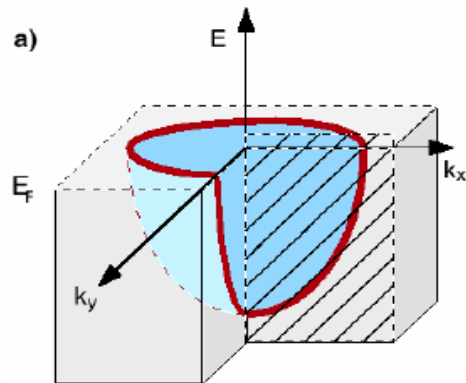
- First experimental work performed by H. Hertz (1886), W. Hallwachs (1888), von Lenard (1900)
- Theoretical explanation by Einstein (1905)

**FIRST EXPERIMENTAL EVIDENCE
FOR QUANTIZATION OF LIGHT!**

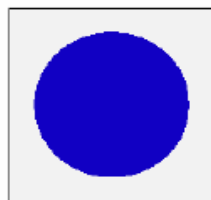
Is there anything else we can learn from the photoelectric effect?

Insights into the solid-state!

Many **properties** of a solids are determined by **electrons near E_F** (**conductivity, magnetoresistance, superconductivity, magnetism**)



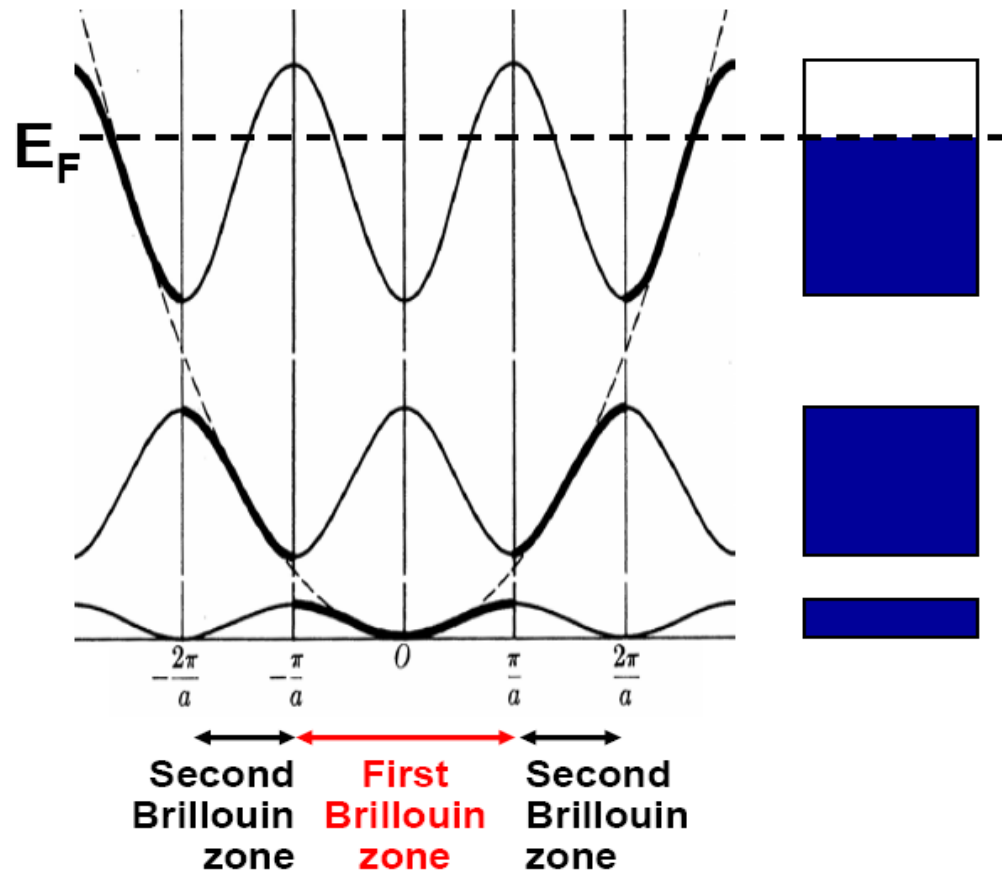
Fermi surface



$n(k)$

Only a **narrow energy slice** around E_F is relevant for these properties (**$kT=25$ meV** at room temperature)

Allowed electronic states Repeated-zone scheme



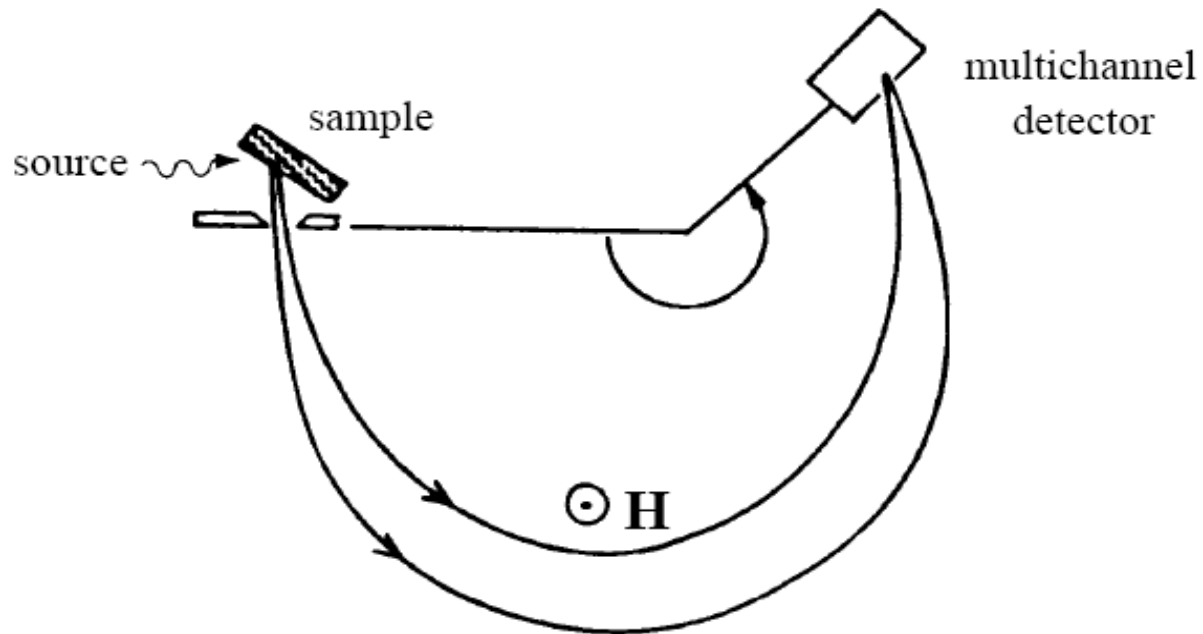
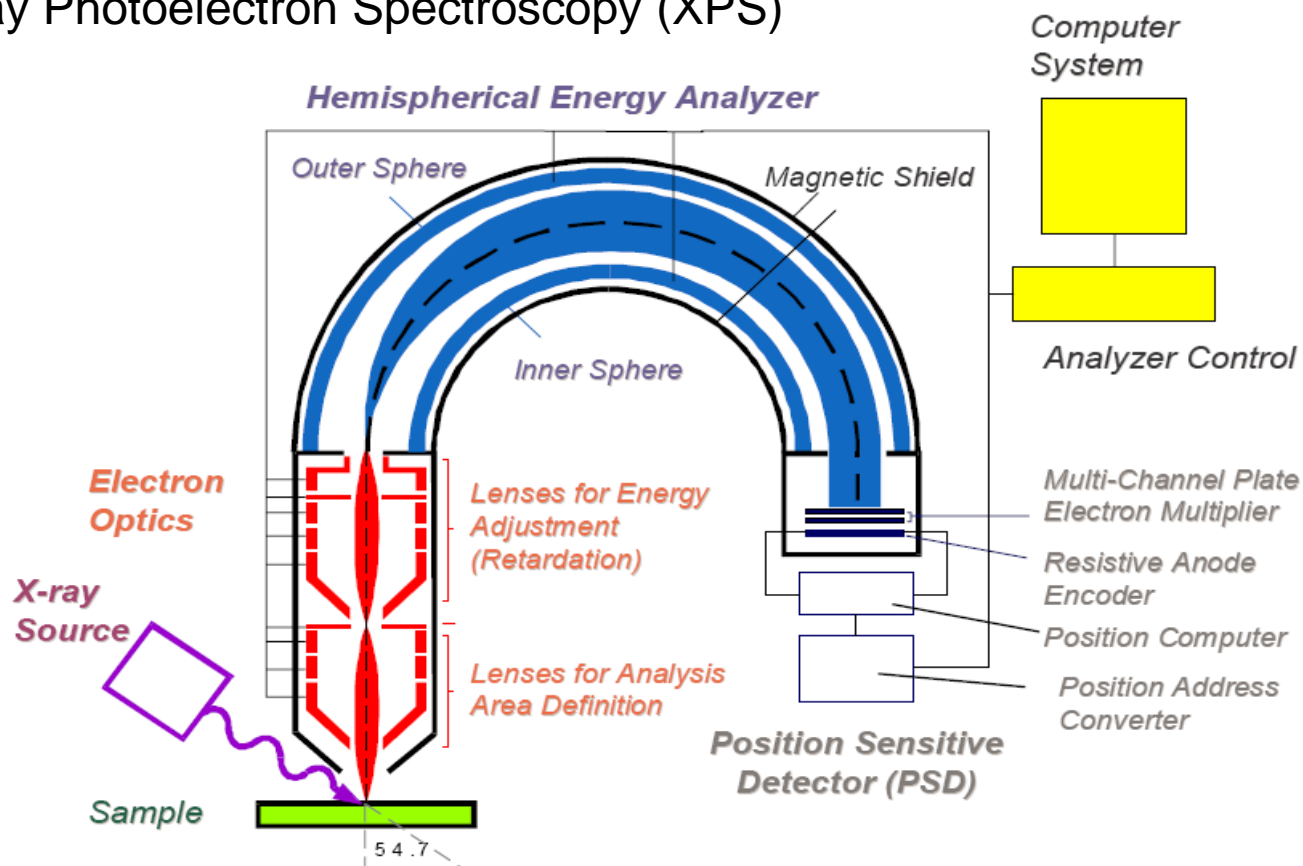
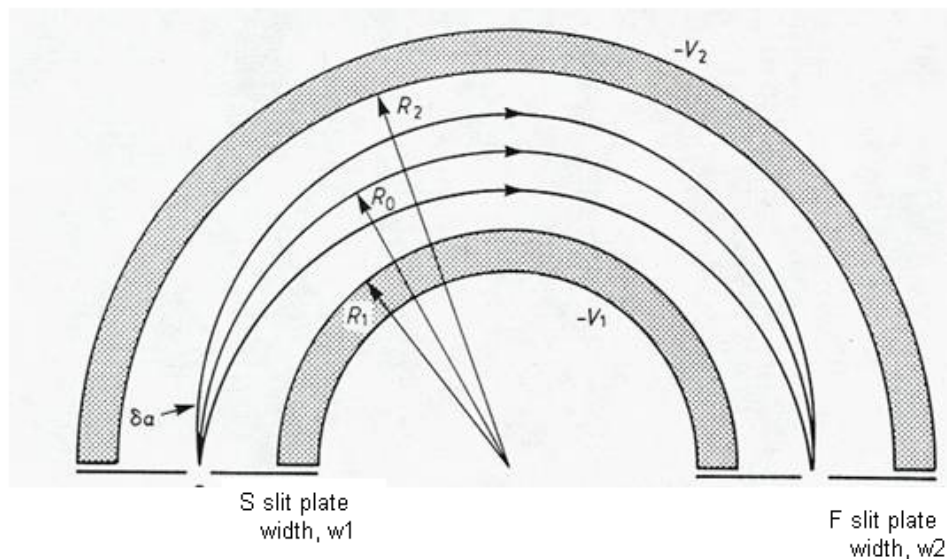


Figure 7.12. Schematic illustration of a photoelectron spectrometer. Photoelectrons emitted from a sample are deflected in roughly circular orbits and focused on a multichannel detector by which their energies are analyzed.

Detection of electrons

X-ray Photoelectron Spectroscopy (XPS)

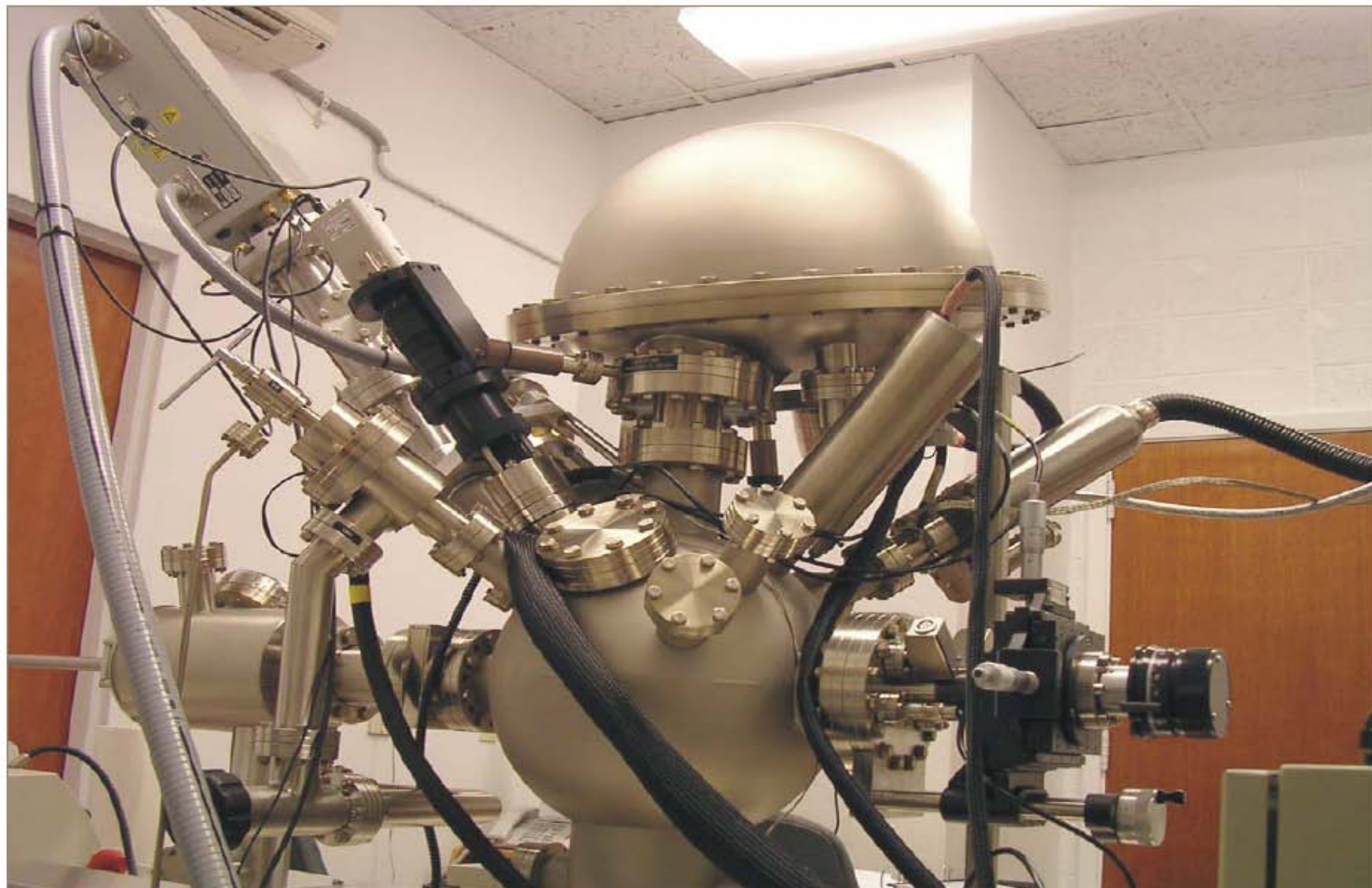




$$V_0 = (V_1 R_1 + V_2 R_2) / 2R_0$$

Schematic cross-section of a concentric hemispherical analyzer (taken from Briggs and Seah)

This means that an electron entering through slit S with a kinetic energy $E = eV_0$ will follow the trajectory through the analyzer along the median equipotential surface of radius R_0 and will be focused at the exit slit, F. Likewise, electrons entering at S with a kinetic energy not equal to eV_0 will follow a different trajectory and will not be focused at F. Because R_0 (equal to 165 mm in Axis 165), R_1 and R_2 are fixed, in principle changing V_1 and V_2 will selectively pass electrons of varying kinetic energies through the analyzer.



The Dalhousie XPS/SIMS system

XPS: VG Microtech MultiLab ESCA 2000 System.

SIMS: Hiden EQS 300 System.

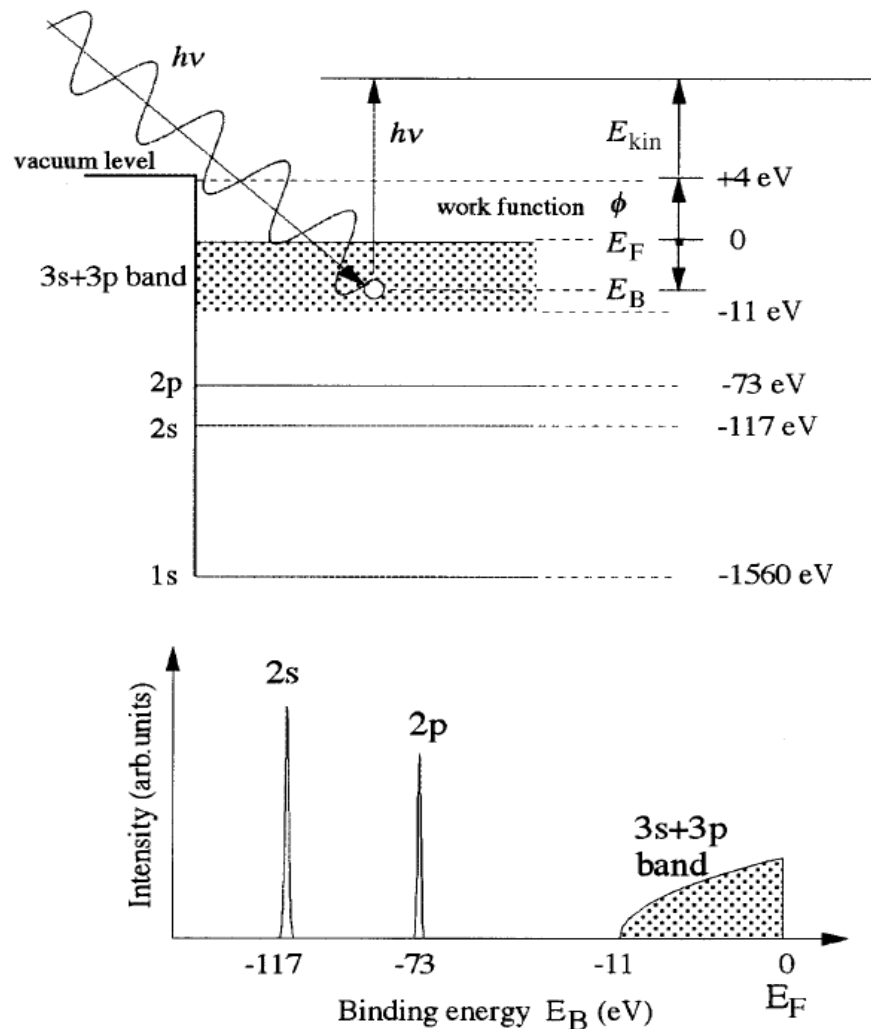


Figure 7.13. Relationship between the electronic structure and the photoemission spectrum. The electronic structure of pure Al is taken as an example. The XPS spectrum is schematically shown in the lower diagram.

The photoemission process comprises three processes:
 (1) electrons are first optically excited to states at higher energy, (2) the photoexcited electrons move through the lattice to the surface of a sample and (3) they escape from the surface into vacuum.

$$E_{kin} = h\nu - \phi - E_B$$

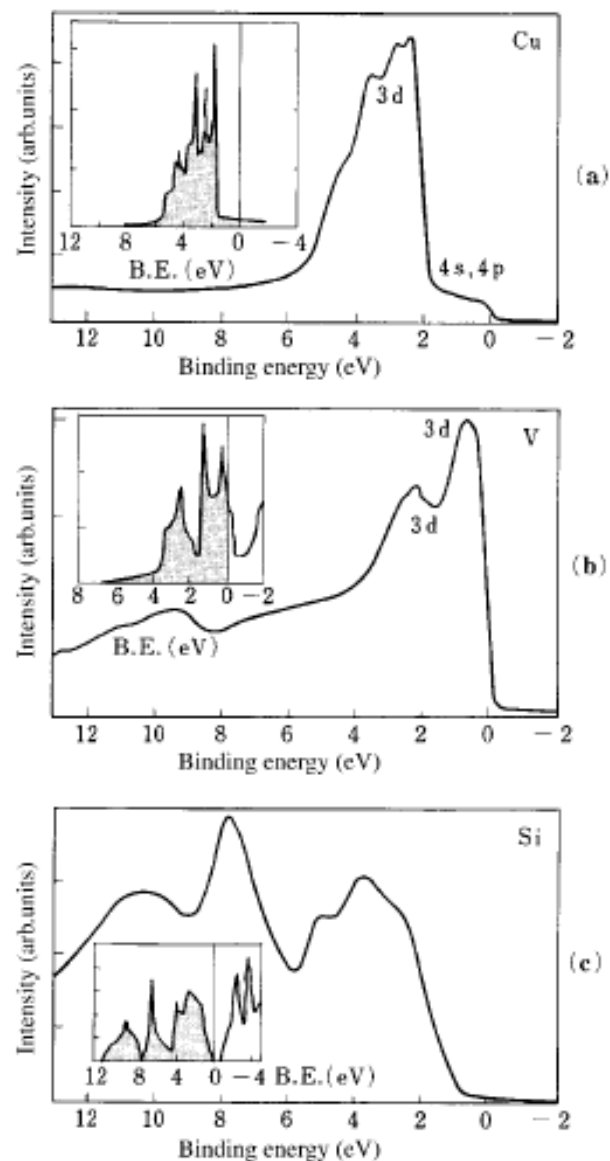


Figure 7.16. XPS valence band spectra for (a) pure Cu, (b) pure V and (c) pure Si. The Fermi level is located at the origin. The XPS apparatus with monochromated Al- $K\alpha$ line is claimed to give a resolution better than 0.25 eV (ESCA-300, Seiko Electronics Industry). Insets show the valence band spectra obtained from band calculations. [V. L. Moruzzi *et al.* *Calculated Electronic Properties of Metals* (Pergamon Press, 1978)]

ARPES

(Angle Resolved PhotoEmission Spectroscopy)

What is ARPES?

- An atomically flat sample is illuminated by a beam of monochromatic light.
- Due to the photoelectric effect, the sample emits electrons.
- The kinetic energy and direction of these electrons are measured by the apparatus.
- This data reflects the structure of the Fermi surface within the material.

Angular-resolved photoemission spectroscopy (ARPES)

The solid angle of detection $\Delta\Omega$ is made small so that photoelectrons in a narrow k -interval only are detected. There are four major parameters in the ARPES experiments: two exit angles ϑ and φ specifying the direction of the photoelectrons, their kinetic energy E_{kin} and the energy of the impinging radiation $\hbar\omega$.

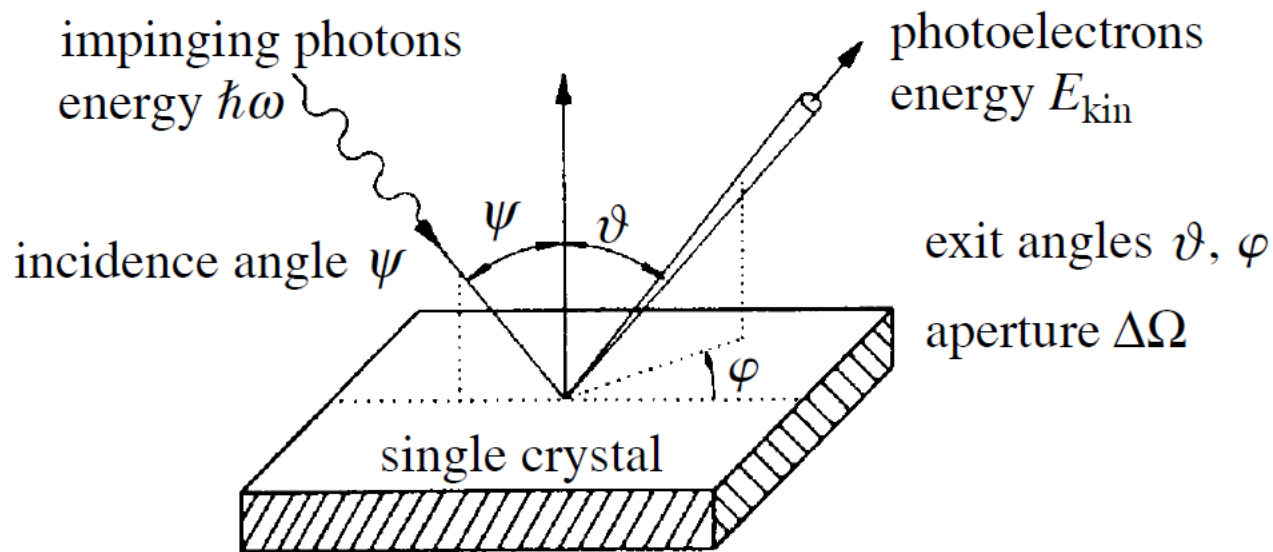
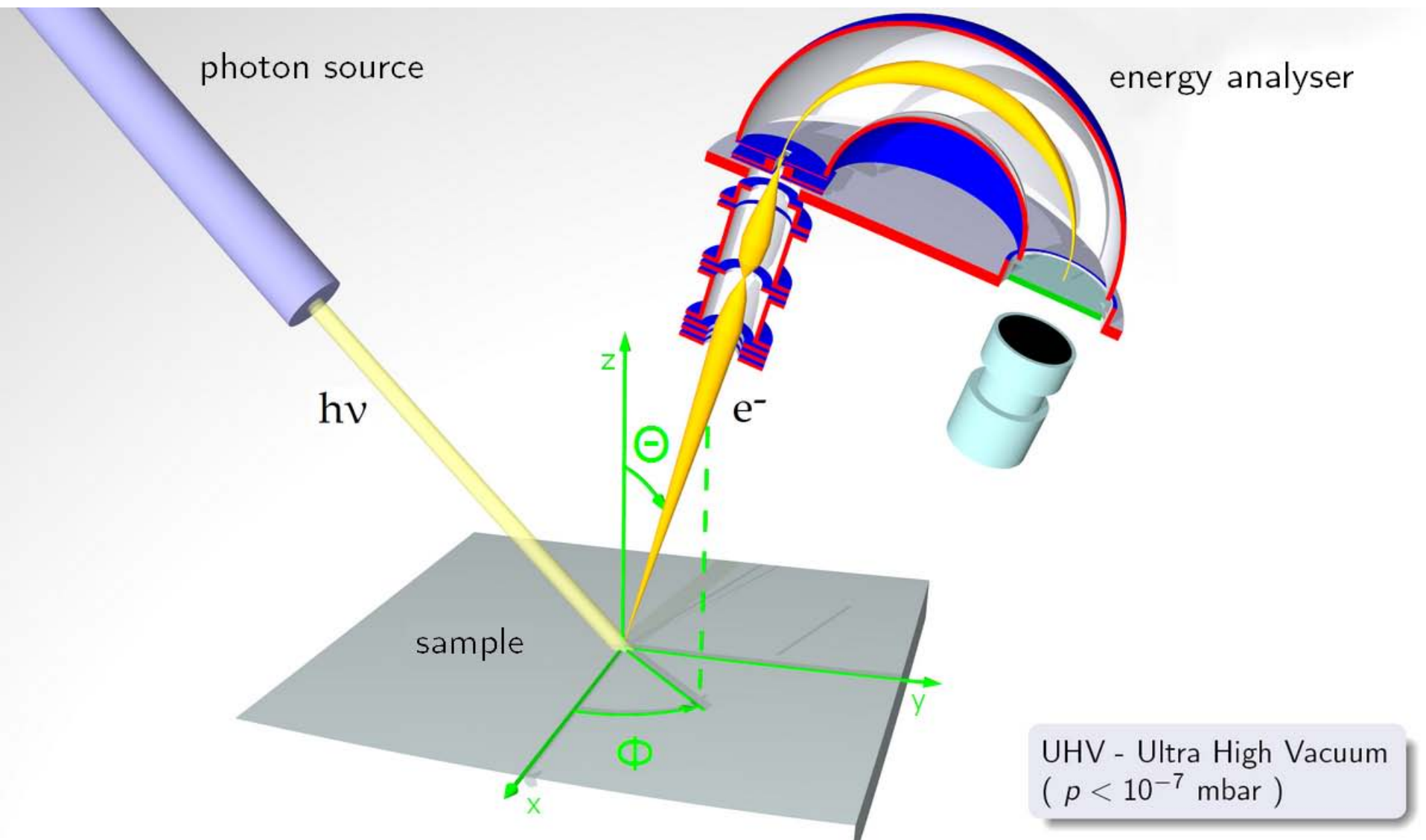
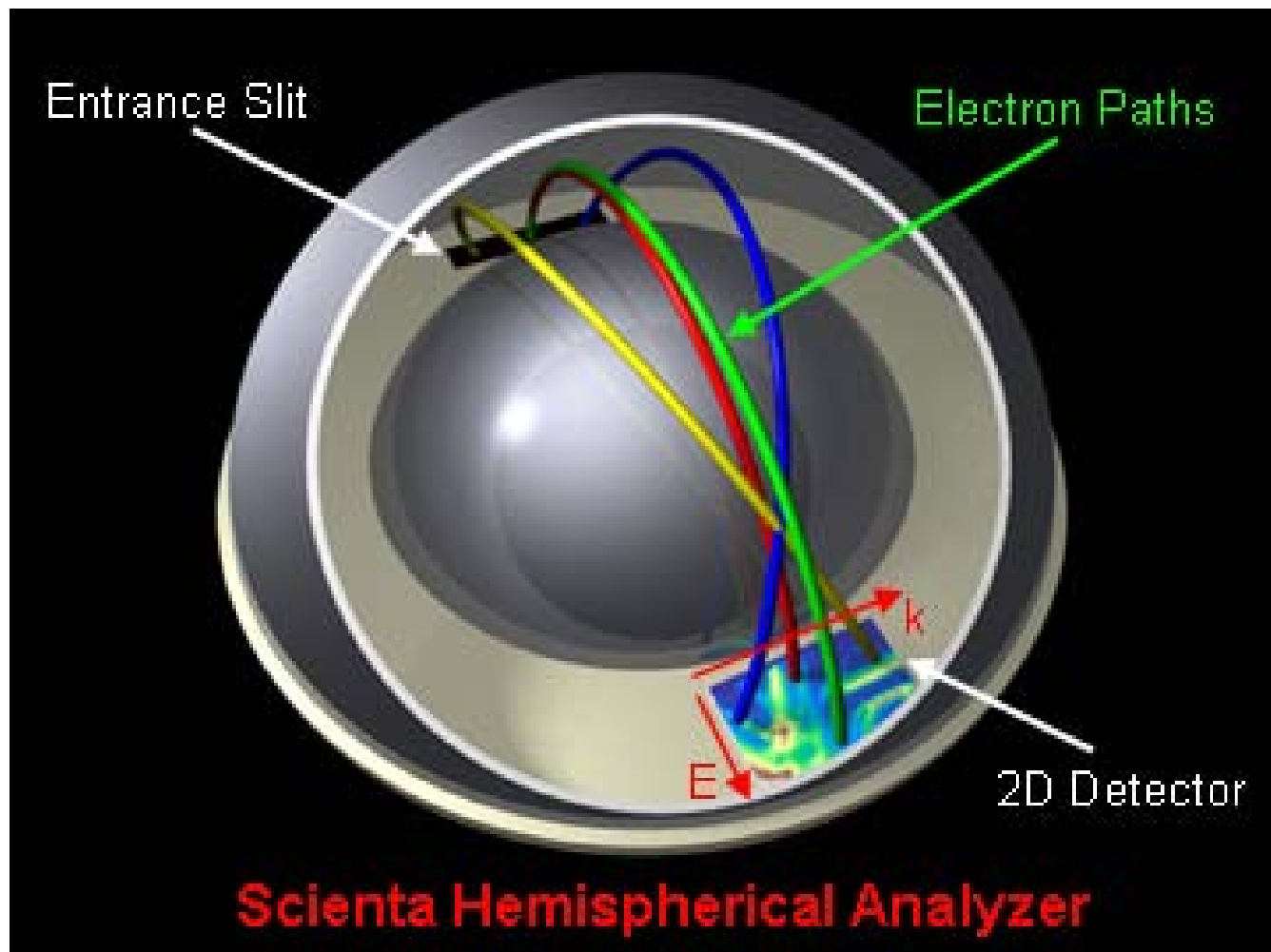


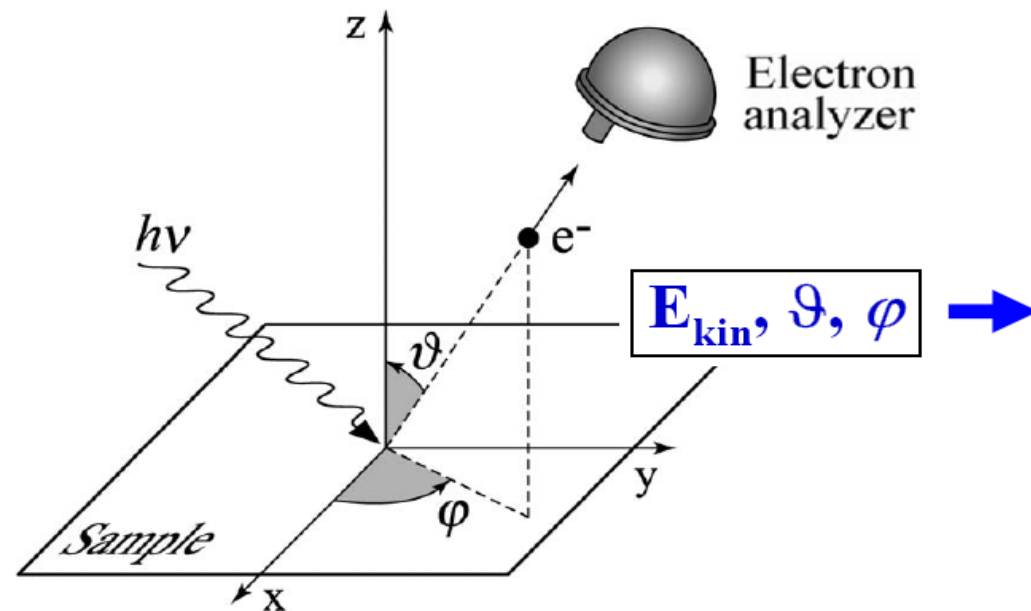
Figure 7.19. Geometry of the ARPES measurements. [S. Hüfner, *Photoelectron Spectroscopy*, Springer Series in Solid State Physics, vol. 82, edited by M. Cardona, (Springer-Verlag, Berlin 1995)]

from Mizutani





http://arpes.stanford.edu/facilities_ssrl.html

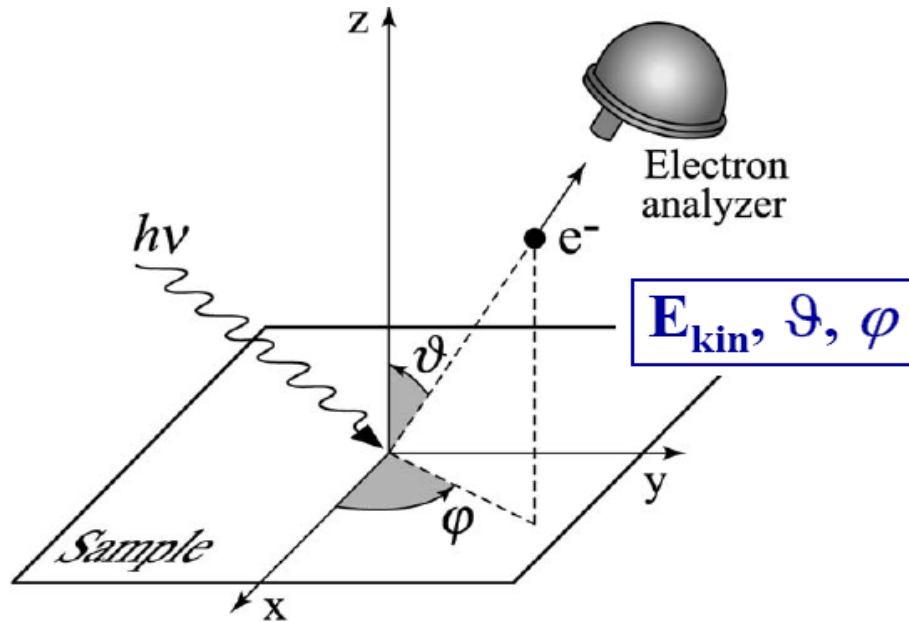


$$\mathbf{K} = \mathbf{p} / \hbar = \sqrt{2m E_{kin}} / \hbar$$

$$K_x = \frac{1}{\hbar} \sqrt{2m E_{kin}} \sin \vartheta \cos \varphi$$

$$K_y = \frac{1}{\hbar} \sqrt{2m E_{kin}} \sin \vartheta \sin \varphi$$

$$K_z = \frac{1}{\hbar} \sqrt{2m E_{kin}} \cos \vartheta$$

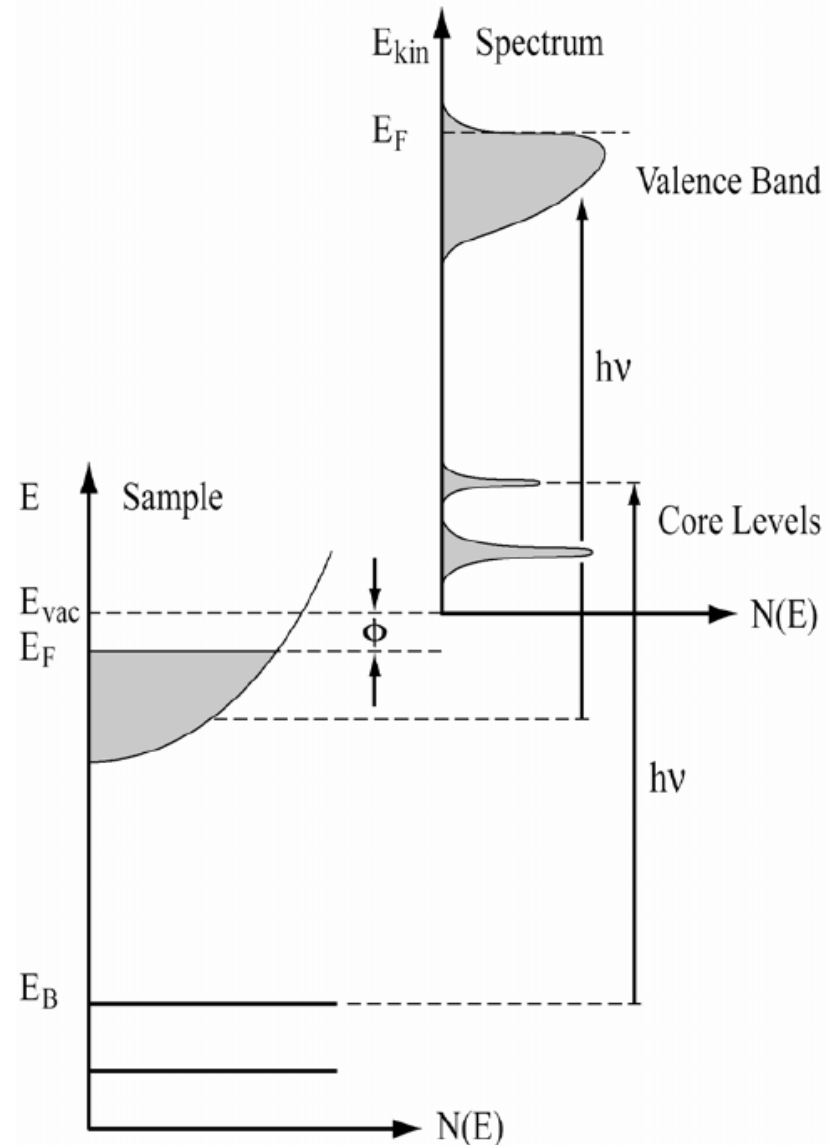


Energy Conservation

$$E_{kin} = h\nu - \phi - |E_B|$$

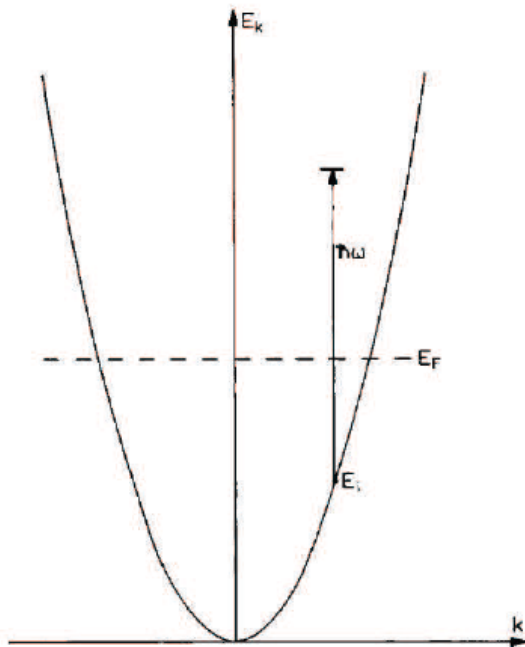
Momentum Conservation

$$\hbar \mathbf{k}_{||} = \hbar \mathbf{K}_{||} = \sqrt{2m E_{kin}} \cdot \sin \theta$$



optical excitation in the solid

assumption: absorption of a photon with energy $h\nu$ leads to a transition between an initial state ψ_i and a final state ψ_f which are both states of the infinite solid



(taken from S. Hufner)

Since the photon momentum is small $|\vec{k}| = 2\pi/\lambda$ such a (direct) transition is not possible for free electrons

. momentum conservation in a crystalline solid

$$\psi_j = u_{\vec{k}}(\vec{r})e^{i\vec{k}\cdot\vec{r}} = u_{(\vec{k}-\vec{G})}(\vec{r})e^{i(\vec{k}-\vec{G})\cdot\vec{r}} \quad \text{Bloch functions}$$

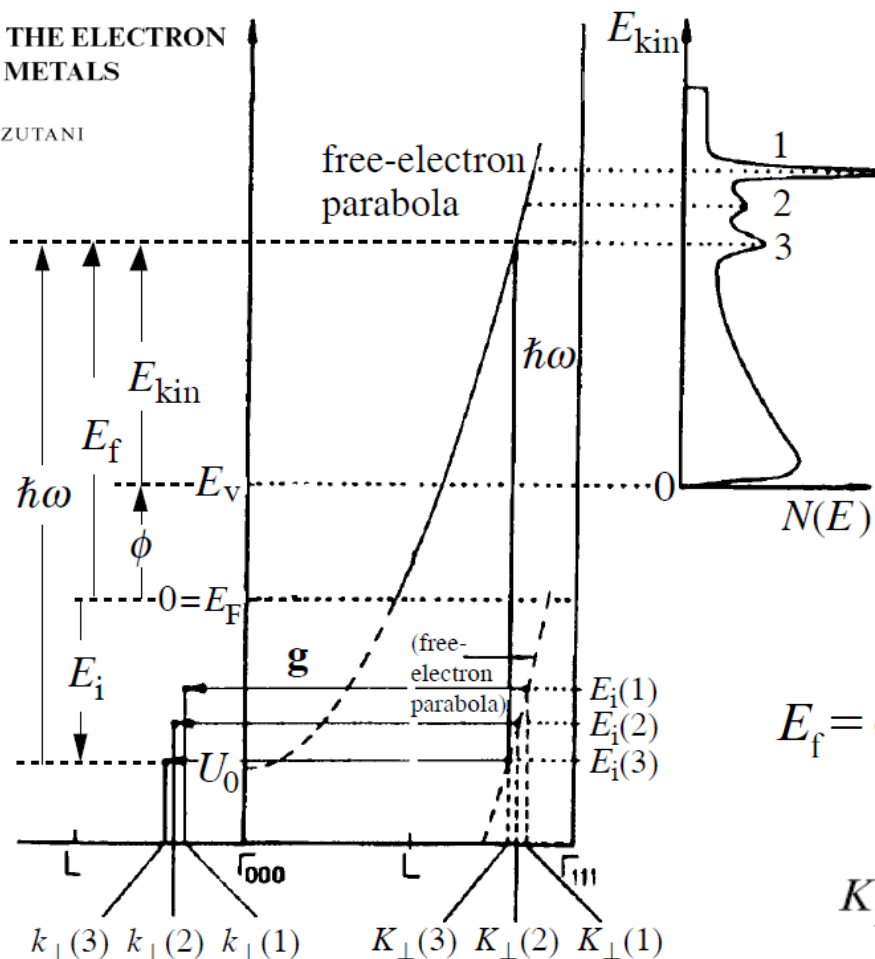
\vec{G} reciprocal lattice vector

From the transition probability:

$$W_{i\rightarrow f} \propto |\langle \psi_f | \mathbf{A} \cdot \mathbf{r} | \psi_i \rangle|^2$$

we obtain for momentum conservation in the solid

$$\vec{k}_i = \vec{k}_f - \vec{G}$$



$$E_f = E_{kin} + \phi$$

$$E_i = E_f - \hbar\omega,$$

$$K_{\parallel}^{pe} = \sqrt{(2m/\hbar^2)E_{kin}} \sin \vartheta = K_{\parallel},$$

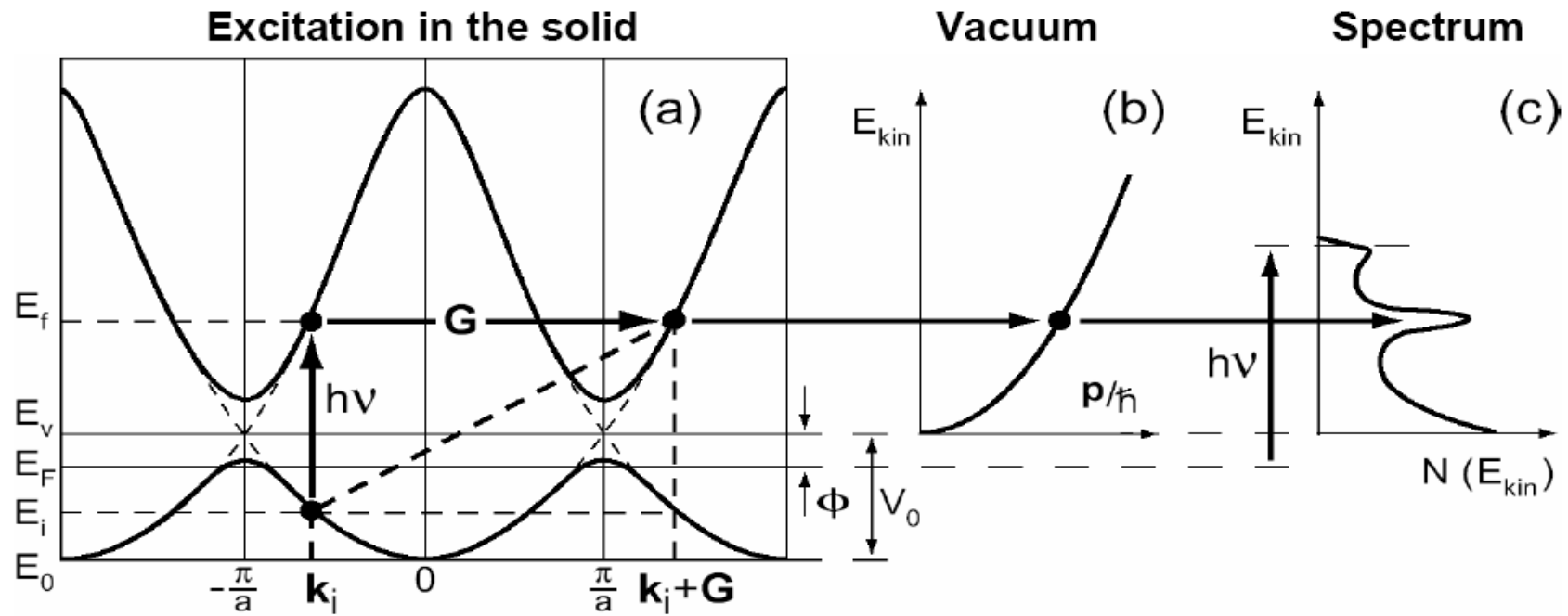
$$-E_i(i) = \hbar\omega - (E_{kin}(i) + \phi)$$

$$E_f = (\hbar^2/2m) (K_{\parallel}^2 + K_{\perp}^2) + U_0$$

$$K_{\perp} = \sqrt{(2m/\hbar^2)(E_{kin} \cos^2 \vartheta + \phi - U_0)}.$$

Figure 7.20. Analysis of the ARPES data by assuming the free-electron model for the final states [7]. See text for detailed description. [S. Hüfner, *Photoelectron Spectroscopy*, Springer Series in Solid State Physics, vol. 82, edited by M. Cardona, (Springer-Verlag, Berlin 1995)]

The full $E-k_{\perp}$ relations in a given direction can be mapped by repeating the same procedure under different incident photon energies $\hbar\omega$ over the range 10 to 100 eV available in the synchrotron radiation experiment.



$$\vec{k}_i = \vec{k}_f - \vec{G}$$

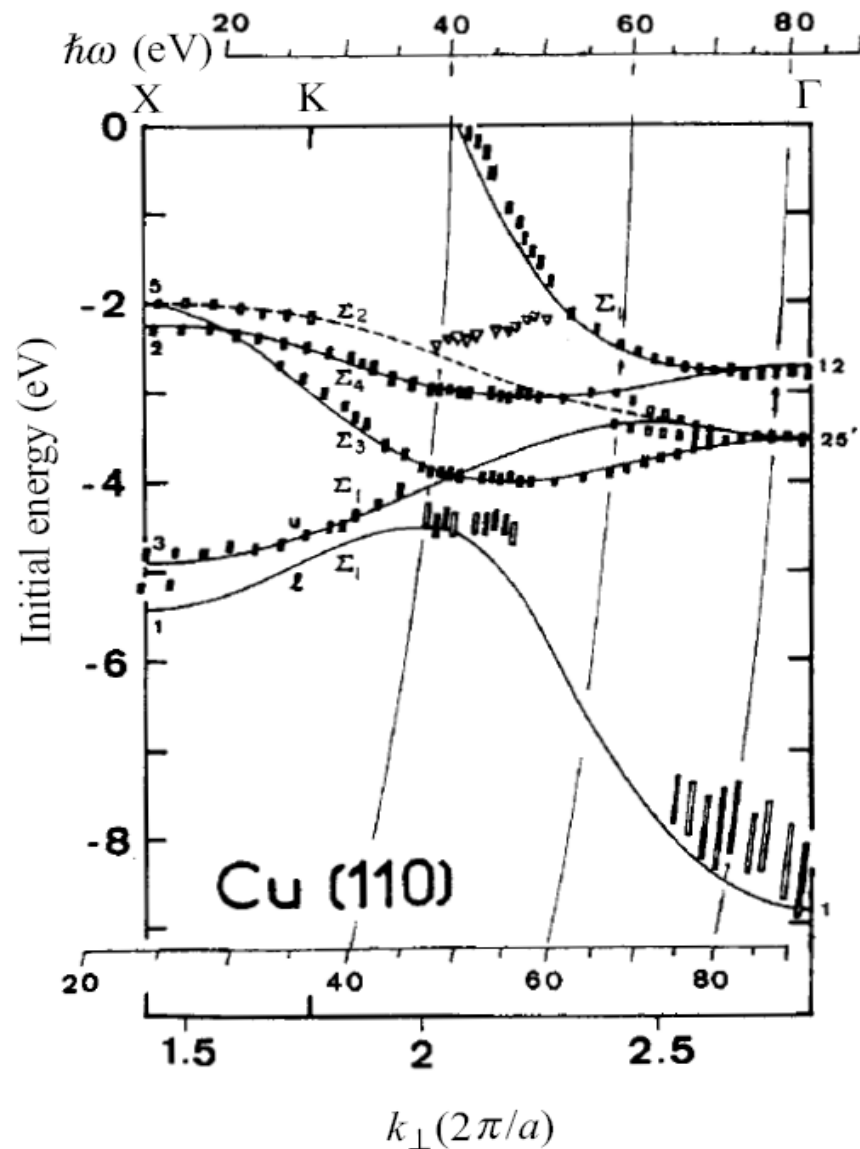


Figure 7.21. Band structure of pure Cu along the $\Gamma K X$ line derived from the ARPES measurements on a (110) crystal surface. The full curve is due to Burdick's band calculations. The height of the rectangle data points indicates experimental uncertainty. Three parabolic curves represent K -dependence of the initial energy $E_i = (\hbar^2 K^2 / 2m) + U_0 - \hbar\omega$. [P. Thiry *et al.*, *Phys. Rev. Lett.* **43** (1979) 82]

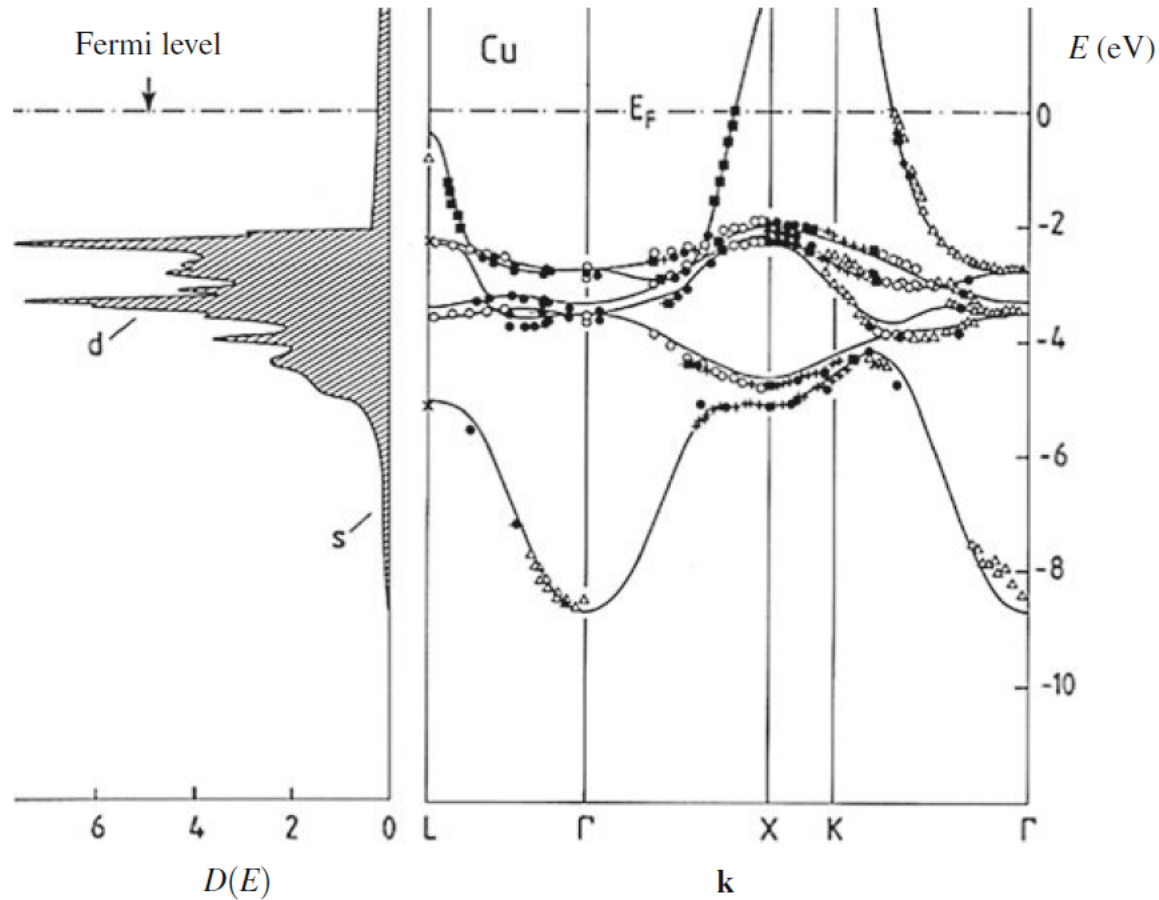
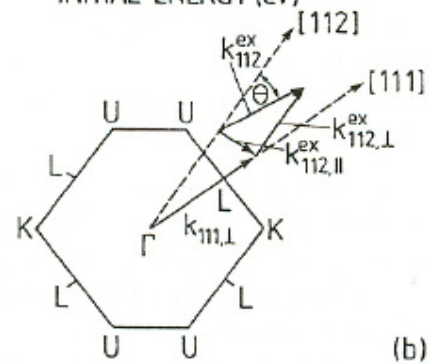
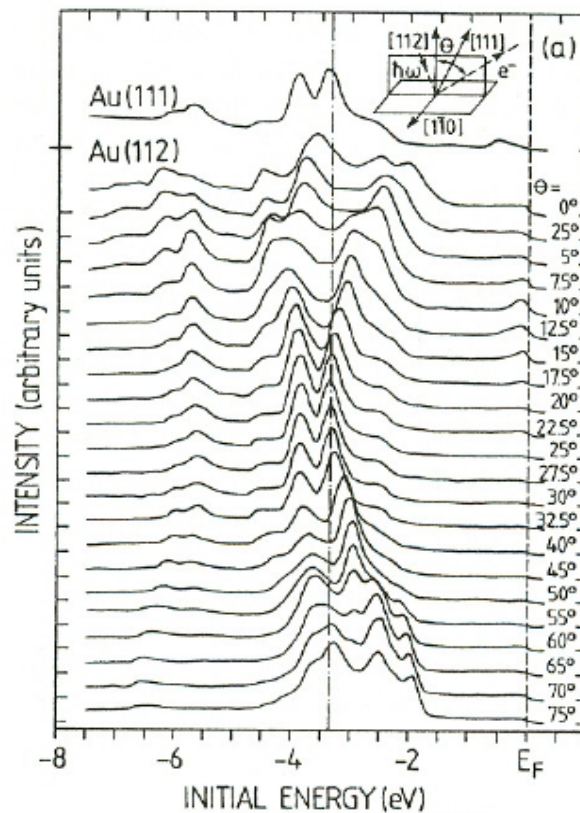
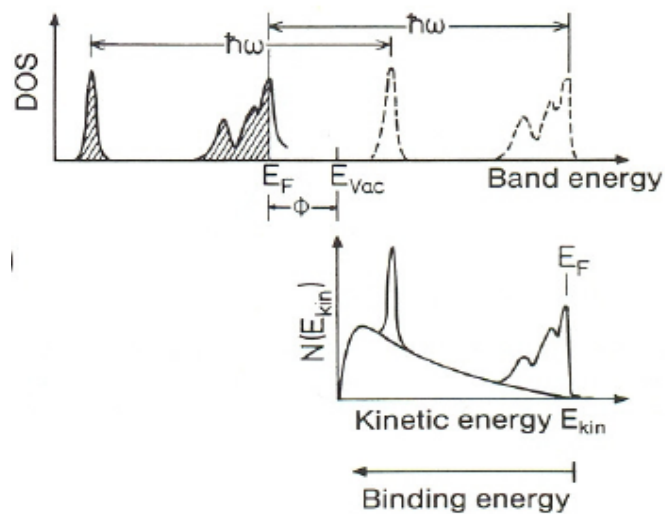


Fig. 3.26 Band structure of valence and conduction electrons of copper, determined by photoemission. The results of numerical simulations are shown by *continuous curves*. The corresponding density of states is shown *on the left*. From [6, p. 145] Springer © 1995. Experimental results from Courths, R., Hüfner, S.: Phys. Rep. **112**, 55 (1984). Band calculation from Eckardt, H., Fritsche, L., Noffke, J.: J. Phys. F **14**, 97 (1984)

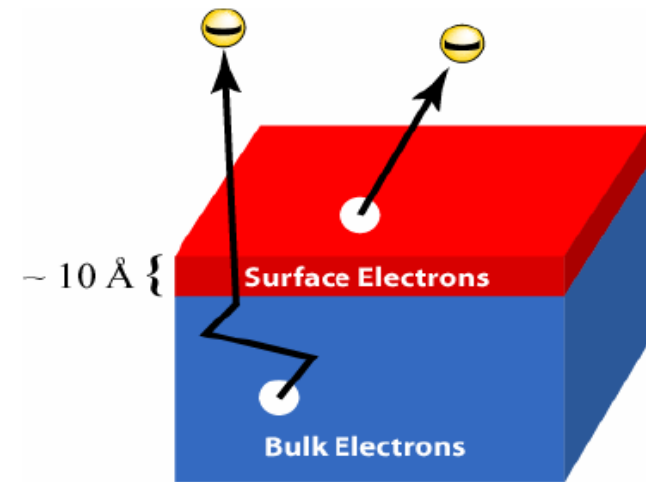


ARPES: Advantages and Limitations

Advantages

- **Direct information about the electronic states!**
- Straightforward comparison with theory - little or no modeling.
- High-resolution information about **BOTH energy and momentum**
- **Surface-sensitive probe**
- Sensitive to “**many-body**” effects
- Can be applied to small samples (100 μm x 100 μm x 10 nm)

Limitations



- **Not bulk sensitive**
- Requires clean, atomically flat surfaces in **ultra-high vacuum**
- Cannot be studied as a function of pressure or magnetic field